CHALMERS

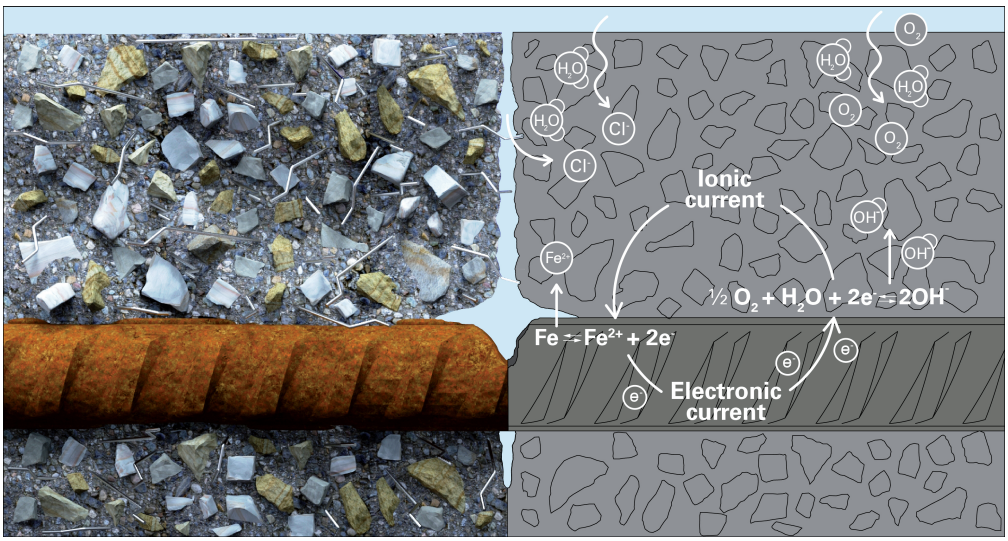

Chloride Induced Corrosion of Steel Bars in Fibre Reinforced Concrete

CARLOS GIL BERROCAL

Department of Civil and Environmental Engineering
Division of Structural Engineering
CHALMERS UNIVERSITY OF TECHNOLOGY
Göteborg, Sweden 2015

THESIS FOR THE DEGREE OF LICENTIATE OF ENGINEERING

Chloride Induced Corrosion of Steel Bars in Fibre Reinforced Concrete

CARLOS GIL BERROCAL

Department of Civil and Environmental Engineering
Division of Structural Engineering
CHALMERS UNIVERSITY OF TECHNOLOGY

Göteborg, Sweden 2015

Chloride Induced Corrosion of Steel Bars in Fibre Reinforced Concrete
CARLOS GIL BERROCAL

Thesis for the degree of Licentiate of Engineering 2015:01
ISSN 1652-9146
Department of Civil and Environmental Engineering
Division of Structural Engineering
Chalmers University of Technology
SE-412 96 Göteborg
Sweden
Telephone: +46 (0)31-772 1000

Cover:
Schematic representation of chloride-induced pitting corrosion on a reinforcing bar embedded in cracked FRC concrete. Figure created by the author in collaboration with Eduard Mondéjar from Matrimoni^{tm} studio (`www.matrimoni.co`).

Chalmers Reproservice
Göteborg, Sweden 2015

Chloride Induced Corrosion of Steel Bars in Fibre Reinforced Concrete

CARLOS GIL BERROCAL
Department of Civil and Environmental Engineering
Division of Structural Engineering
Chalmers University of Technology

Abstract

Chloride-induced corrosion of reinforcement is the most widespread degradation mechanism affecting the durability of reinforced concrete structures. Macro-cracks provide a preferential path for moisture, oxygen and Cl^- ions to reach the embedded reinforcement, playing a major role in their total transport. Therefore, to effectively control macro-cracking is essential with respect to the service life. Fibre reinforcement, even at low dosages, leads to arrested crack development, also in conventionally reinforced concrete. Thus, it could be advantageous to use fibres in civil engineering structures where their crack limiting effect is of interest. However, despite the increased corrosion resistance of steel fibres, the use of both types of reinforcement in chloride environments raises questions.

The present study aimed at investigating the viability of employing fibre reinforcement to improve the durability performance of conventionally reinforced concrete structures with respect to delayed and/or reduced corrosion by controlling the development of cracks. The work includes long-term experiments of naturally corroded concrete elements with and without fibres, in sound and cracked state, subjected to different loading conditions and various crack widths. Complementary material tests to study the influence of fibres on different properties governing the corrosion of steel reinforcement in concrete were also carried out. Additionally, experiments were started to determine the possible formation of galvanic cells between metallic fibres and steel bars.

The results showed that while the electrical resistivity of concrete was unavoidably reduced by the presence of steel fibres, the ingress of chloride, assessed through migration and bulk diffusion tests, was not significantly affected. The analysis of the corrosion initiation period in cracked specimens revealed that, when loaded to reach the same surface crack width, fibre reinforced specimens performed similar or better than their plain concrete counterparts. However, the improvement achieved by adding fibres was, in general, minor compared to the results obtained for uncracked specimens, highlighting the utmost importance of cracks for the initiation of corrosion. Accordingly, corrosion initiated almost immediately in specimens subjected to a sustained load, i.e. with open cracks, regardless of the presence of fibres. This observation indicated the existence of a critical crack width above which the initiation period could be, in practice, disregarded.

Questions that remain unclear and that require further research include: (i) the influence of reduced electrical resistivity on the corrosion rate of rebar; (ii) the risk of galvanic corrosion caused by the different steels used for fibres and bars; and (iii) the effectiveness of fibres to control the development of corrosion-induced cracks and spalling of the concrete cover. Forthcoming results from the experiments developed during this project, which are still ongoing, are expected to shed some light on these questions.

Keywords: Fibre reinforced concrete, chloride-induced corrosion, reinforced concrete durability, crack width, chloride ingress, electrical resistivity

to Maria & Marcos

Preface

The work presented in this licentiate thesis was initiated as the result of the fruitful collaboration between Chalmers University of Technology and AB Färdig Betong and Thomas Concrete Group, preceded by the works conducted by Ingemar Löfgren and later by Anette Jansson on fibre reinforced concrete structures. The present work was carried out between December 2012 and January 2015 in the research group of Concrete Structures within the Diviosion of Structural Engineering at Chalmers University of Technology.

First, I would like to thank my supervisors, Prof. Karin Lundgren and Adj. Prof. Ingemar Löfgren, for the trust they put in me in the first place, but also for their continuous encouragement, advice and guidance as well as for providing valuable discussion and enlightening me with their deep knowledge. I would also like to thank Prof. Luping Tang for assisting me throughout the different stages of this work and sharing his vast experience in chloride ingress and corrosion of steel in concrete.

I want to convey my appreciation to the rest of members of the reference group, Anders Lindvall, Elisabeth Helsing, Per-Ola Svahn, Mikael Westerholm, Arvid Hejll and Claus K. Larsen, for showing their interest in my work and taking the time to get involved and share their valuable thoughts and comments.

I would also like to thank all my colleagues, former and present, at the Division of Structural Engineering for creating such a nice working environment. Special thanks go to Filip Nilenius, my office mate for several months, for his support and constant help with LaTeX, to Jonas Ekström, my *mentor*, for informal discussions and practical help and to Ignasi Fernandez for his valuable assistance during his stay at Chalmers. I want to thank as well, Emma and Arezou from the Division of Building Technology, for their kind predisposition to help me in the lab whenever was needed. I am also grateful to the technical staff at Chalmers, Lars Wahslström, Marek Machowski and Sebastian Almfeldt, for their help in executing the experimental work.

I would like to express my gratitude to Thomas Concrete Group and AB Färdig Betong for making this project possible through financial support. Furthermore I would like to acknowledge *MaxFrank* and *Cementa Research* for their selfless contribution to the project.

Last, but not least, I want to thank all my friends and, particularly, Jacinto and Eduardo for their encouragement and moral support and Eduard and Xenia for inspiring discussion and contribution to the cover of this thesis. Finally, I am deeply grateful to my family for their support and understanding of the implications of being a PhD student.

Thesis

This thesis consists of an extended summary and the following appended papers:

Paper I C. G. Berrocal, K. Lundgren, and I. Löfgren. *Corrosion of Steel Bars Embedded in Fibre Reinforced Concrete Under Chloride Attack: State-of-the-Art.* Submitted to "Cement and Concrete Research"

Paper II C. G. Berrocal, I. Löfgren, K. Lundgren, and L. Tang. *Corrosion Initiation in Cracked Fibre Reinforced Concrete: Influence of Crack Width, Fibre Type and Loading Conditions.* Submitted to: "Corrosion Science"

Author's contribution to jointly written papers

The appended papers were prepared in collaboration with the co-authors. In the following, the contribution of the author of this licentiate thesis to the appended papers is described.

In **Paper I** the author participated in the planning of the paper, made the literature study, contributed to the discussion of the results and took the major responsibility for the writing of the paper.

In **Paper II**, the author made the literature study, participated in the planning and execution of the experimental programme, carried out the analysis of the data, participated in the discussion of the results and took responsibility for the planning and writing of the paper.

Other publications related to the thesis

In addition to the appended papers, the author of this thesis has also contributed to the following publications:

Berrocal, C. G., Lundgren, K., and Löfgren, I. (2013). "Influence of Steel Fibres on Corrosion of Reinforcement in Concrete in Chloride Environments: A Review". In: *7th International Conference: Fibre Concrete 2013*. Ed. by A. Kohouyjova. Prague, Czech Republic, pp. 1–10.

Berrocal, C. G., Löfgren, I., and Lundgren, K. (2014). "Experimental Investigation on Rebar Corrosion in Combination with Fibres". In: *Proceedings of the XXII Nordic Concrete Research Symposium*. Ed. by The Nordic Concrete Federation. Reykjavik, Iceland: Norsk Betongforening, pp. 223–226.

Contents

Abstract **i**

Preface **v**

Thesis **vii**

Author's contribution to jointly written papers **vii**

Other publications related to the thesis **viii**

Contents **ix**

1 Introduction **1**
1.1 Background 1
1.2 Aim and scope 3
1.3 Scientific approach 4
1.4 Limitations 4
1.5 Outline of the thesis 4

2 Theoretical Framework **6**
2.1 Corrosion of reinforcement bars in concrete 6
2.2 Influence of cracking on corrosion 9
2.3 Fibre reinforced concrete 10

3 Overview of Experimental Programme **12**

4 Long-Term Corrosion Tests **14**
4.1 Experimental work review 14
4.2 Discussion of parameters 18
4.2.1 Specimen characteristics 19
4.2.2 Fibre reinforcement 21
4.2.3 Exposure conditions 23
4.2.4 Loading conditions 26
4.3 Description 28
4.3.1 Specimen design and materials 28
4.3.2 Casting and curing 29
4.3.3 Pre-loading procedure 31
4.3.4 Sustained loading set-up 31
4.3.5 Exposure conditions 33
4.3.6 Corrosion measurements 35

5 Material Tests **40**
5.1 Compressive strength . . . 40
5.2 Flexural tensile strength . . . 41
5.3 Electrical resistivity . . . 41
5.4 Chloride diffusion coefficient . . . 42
5.4.1 Non-steady state migration test . . . 42
5.4.2 Bulk diffusion test . . . 43

6 Galvanic Corrosion Tests **45**
6.1 Description . . . 45
6.1.1 Test configuration . . . 46
6.1.2 Specimen design and materials . . . 47
6.1.3 Specimen preparation . . . 48
6.1.4 Exposure conditions . . . 49
6.1.5 Evaluation . . . 49

7 Results **50**
7.1 Material tests . . . 50
7.1.1 Compressive strength . . . 50
7.1.2 Flexural tensile strength . . . 50
7.1.3 Electrical resistivity . . . 51
7.1.4 Chloride migration coefficient . . . 53
7.1.5 Chloride diffusion coefficient . . . 53
7.2 Long-term corrosion experiments . . . 56
7.2.1 Half-cell potential monitoring . . . 56
7.2.2 Corrosion initiation times . . . 56
7.2.3 Corrosion rate . . . 61
7.2.4 Corrosion of steel fibres . . . 62
7.3 Modelling of chloride ingress . . . 64
7.4 Concluding discussion . . . 67

8 Conclusions **68**
8.1 General conclusions . . . 68
8.2 Suggestions for future research . . . 69

References **71**

Appendix A: Half-cell potential measurements **79**

Paper I **89**

Paper II **125**

Extended Summary

1 Introduction

1.1 Background

Reinforced concrete (RC) is nowadays present in a large part of the infrastructure all over the world. The high compressive strength of concrete combined with the tensile properties of steel makes it a competitive and versatile material suitable for a multitude of applications. Existing structures made of RC include, for instance, bridges, tunnels, harbours, dams or off-shore platforms, as well as a wide range of buildings. It is precisely due to this broad variety of applications that reinforced concrete structures are often exposed to extremely severe conditions, e.g., marine environment, freeze-thaw cycles, carbon dioxide, chemical and biological attack, etc.

Corrosion, due to chlorides present in sea water and in most of the de-icing salts used to remove ice and snow from the roads, is today regarded as one of the biggest problems affecting the durability of RC structures (Hobbs 2001). Corrosion of reinforcing steel is avoided in the first place because it entails the appearance of surface cracks and rust stains giving a bad aesthetic impression. However, if corrosion proceeds, it may lead to a serious loss of the local cross-sectional area of the reinforcing bars and a reduction of the bond between the concrete and the steel, both of which affect the structural behaviour of the RC element and which may eventually compromise the stability and safety of the structure. During the last century a number of structural failures have occurred the causes of which have been mainly attributed to corrosion problems (Bertolini et al. 2004).

The problems associated with corrosion are not merely structural. Most existing civil engineering structures have been designed for a total life-span ranging from 50 to 100/120 years.Yet it is not unusual to find structures that have incurred severe damage after only 15 to 20 years from the start of their service life. Therefore, traffic administrations from countries the structures of which suffer from corrosion damage are putting a great deal of effort into repairs, retrofitting and replacements of these structures to avoid additional incidents. Unfortunately, all these actions represent a huge economical cost to society in order to maintain an adequate state of serviceability in the current civil engineering infrastructure.

The increased awareness of the problems and costs that can be directly attributed to the corrosion of reinforcement has spurred research into new methods to delay, reduce or even prevent corrosion. Current methods are very diverse in nature and focus on different aspects of the corrosion process to mitigate its effects. Corrosion inhibitors, for instance, are chemical compounds which can be added to the concrete mixture or applied

onto the surface of hardened concrete to disrupt the anodic and cathodic partial reactions occurring at the rebar surface. Cathodic protection provided by the supply of an external current or the use of sacrificial anodes can be also used. Steel reinforcement bars with a surface treatment, e.g. epoxy coated or galvanized, also represent a common way to mitigate corrosion. Even the use of alternative reinforcing materials with improved corrosion resistance, e.g. stainless steel or non-corroding materials, such as Fibre Reinforced Polymer, have been investigated (Broomfield 2002).

However, the use of any of the aforementioned preventive methods, irrespective of the method chosen, often leads to the rise of secondary problems, such as chemical incompatibilities with the concrete, the need for additional equipment, a loss of mechanical properties or prohibitive costs. Nevertheless, whether these methods could in practice mitigate the effects of corrosion on reinforced concrete structures in an effective way, they all share the common feature of being very specific to the problem, i.e. no beneficial effects are gained other than improved corrosion resistance. An ideal method would not only mitigate corrosion effectively, but would also provide mechanisms to improve its structural behaviour (Blunt 2008).

The degradation process of reinforced concrete is governed by transport mechanisms that allow the ingress of detrimental substances found in the environment towards the inner zones of concrete where the reinforcement is located. Therefore, preventive methods should never be used as substitutes for good quality, well-executed and well-cured concrete (Geiker 2012). Large concrete covers are also a desirable parameter to slow down the ingress of deleterious agents and thus obtain more durable structures. On the other hand, the use of large concrete covers implies that cracks formed at the concrete surface can develop without impediments until they reach the reinforcement, resulting in large surface crack widths. Cracks are regarded as potentially harmful to the corrosion process, as they provide preferential paths for external agents to penetrate into concrete. Current structural codes (EN 1992-1-1 Eurocode 2 2004; *fib Model Code for Concrete Structures* 2010; ACI Committee 318 2011) specify crack width limitations which may be fulfilled using small bar diameters and placing additional amounts of secondary reinforcement with narrow spacing. This practice, though, tends to cause congested reinforcement layouts which complicate the casting and vibrating procedure of concrete structures, leading to potential defects that may ultimately impair the durability of a structure.

Fibre reinforced concrete (FRC) has been successfully used in a number of applications, mainly buildings, pavements and slabs on grade to arrest cracking, mostly due to plastic and drying shrinkage (Löfgren 2005), but also in tunnels as sprayed concrete (Nordström 2005) or precast segmental linings (de la Fuente et al. 2012) and due to their improved water tightness as containment structures (Vitt 2008). Therefore, it is argued that fibres could also be used in civil engineering structures like bridges or harbour piers, where their limiting crack effects are of interest, to decrease the ingress of detrimental agents, thus reducing or even preventing the corrosion of reinforcement.

1.2 Aim and scope

The aim of the present work is to investigate the viability of using fibre reinforcement to improve the durability performance of cracked reinforced concrete elements in terms of delayed and/or reduced corrosion by controlling the development of cracks. To reach the general aim, the following specific objectives have been defined:

- To understand how fibres might influence the properties of the concrete that are relevant to the corrosion process of steel reinforcement, e.g water permeation, ion diffusion, electrical resistivity.
- To study how the corrosion of reinforcement might be influenced in concrete elements subjected to different loading conditions and varying surface crack widths.
- To investigate how the corrosion initiation and propagation might be affected by the addition of fibres into concrete in either sound or cracked state.
- To identify the challenges of using fibre reinforcement in general and steel fibres in particular in conventionally reinforced concrete structures prone to suffering chloride-induced corrosion.

Although not answered in this thesis, additional objectives were defined to meet the overall aim of the project. The following objectives were also considered in this project, especially in the design of the experiments, and will be investigated in the remaining part of the work:

- To assess the effectiveness of fibre reinforcement to arrest the development of corrosion-induced cracks in conventionally reinforced concrete elements.
- To quantify the influence of fibre reinforcement on the corrosion rate of conventional rebar in cracked and sound concrete specimens.
- To assess, quantitatively, the extent to which fibres may influence the damage caused by corrosion, in terms of maximum corrosion penetration and bond degradation due to the spalling of concrete.
- To identify the risk of galvanic cell formation between various metallic fibres and steel reinforcing bars.

1.3 Scientific approach

An extensive literature study was conducted to compare and analyse the experimental data available in the literature and thus identify how the addition of fibre reinforcement may influence concrete in terms of the properties governing the corrosion process, e.g. cracking behaviour, water permeation, chloride diffusion and electrical resistivity.

In parallel, an experimental programme was designed and executed in order to investigate the aims stated. The programme included a principal experiment type involving the long-term monitoring of reinforced concrete elements, with varying fibre types or no fibres, exposed to a chloride rich environment and a second experiment type to investigate the potential galvanic cell formation between fibres and conventional reinforcement bars. Complementary material tests, according to current standards, were carried out to assess the influence of fibres on both the mechanical and transport properties of concrete.

1.4 Limitations

Most limitations in this study are direct results of the choices and decisions made during the planning phase of the experimental programme. In this case, parameters such as the w/c ratio or the concrete cover, which are well-known to play a fundamental role in protecting steel bars from the external agents, were not considered variables. Only chloride-induced corrosion was investigated, hence the effect of carbonation was not considered. Despite the large variety of available fibres in the market combining different features of the material, length, aspect ratio or shape, only three types of fibres were chosen to be tested during this investigation. As for the conventional reinforcement, only B500B steel Ø10 mm ribbed bars were investigated, which were used as received, i.e. without applying any surface treatment. Due to time limitations, only corrosion initiation will here be discussed. However, the experiments described in this thesis are continuing and further results regarding the corrosion propagation period and galvanic corrosion are expected to be obtained in the future.

1.5 Outline of the thesis

This thesis consists of an introductory part and two appended papers.

Chapter 2 introduces the fundamental knowledge necessary to establish the theoretical framework on which this project has been developed. In Paper I, this knowledge is extended through a literature review on how the corrosion of reinforcement may be influenced by using steel fibres in conventionally reinforced concrete structures exposed to chloride environments.

Chapter 3 presents an overview of the experimental programme in which the different types of experiments considered are listed and the types of results, either available at the time or expected for the future, are mentioned.

Chapter 4 gives a detailed description of the main type of experiment conducted during this project, motivating the choices made during the planning phase.

In Chapter 5 and Chapter 6, the material tests and galvanic corrosion experiments are described, respectively.

Chapter 7 and Paper II present results on corrosion initiation in cracked concrete beams, with or without fibre reinforcement, subjected to various loading conditions. The main findings are highlighted and discussed. Results from the material tests are also presented and discussed.

In Chapter 8, the main conclusion from this study are drawn and suggestions for future research are given.

2 Theoretical Framework

2.1 Corrosion of reinforcement bars in concrete

The phenomenon of corrosion is an electrochemical process (Page and Treadaway 1982) which can be understood as two half-cell reactions, anodic and cathodic reactions, taking place between the surface of a metal and the environment with which it is contact, in the presence of moisture. In the case of steel reinforcement, these reactions can be described using Eq. (2.1), which represents the anodic oxidation of iron and the cathodic reduction of oxygen. Both of these reactions happen simultaneously and are necessary for the continuation of the corrosion process.

$$\begin{aligned} Fe &\rightarrow Fe^{2+} + 2e^- \\ H_2O + \tfrac{1}{2}O_2 + 2e^- &\rightarrow 2OH^- \end{aligned} \tag{2.1}$$

A Pourbaix diagram (Pourbaix 1973) is a graphical representation of the thermodynamically stable regions of an aqueous electrochemical system for different potential and pH combinations according to the Nernst's equation. Fig. 2.1 illustrates the Pourbaix diagram for iron, *Fe*, in which three different thermodynamic corrosion regions can be identified: an immunity region, a passivity region and an active corrosion region.

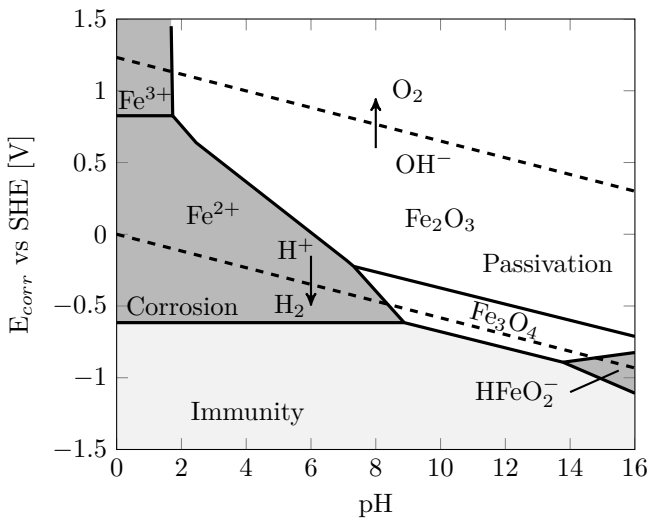

Figure 2.1: *Simplified Pourbaix diagram for iron in water at* 25 °C *(ion activity* $1 \times 10^{-6}\,\mathrm{mol\,l^{-1}}$*) (Pourbaix 1973)*

From this diagram it can be observed that at very low potentials, the steel is in the immunity region, which means that corrosion is not thermodynamically favored. When

potentials increase, for very high pH values, as is the case with the pore solution of the concrete, the steel is in the passivity region. This means that under high alkalinity conditions, a very thin, dense and stable iron-oxide film is formed on the surface of the steel (Ghods 2010). This film, often referred to as the passive layer, greatly reduces the ion mobility between the steel and sorrounding concrete; thus, the rate of corrosion drastically drops and becomes negligible. Therefore, under most conditions, well designed and executed reinforced concrete structures will present good durability as the concrete provides protection against the corrosion of reinforcing steel.

Nevertheless, corrosion remains one of the major problems affecting reinforced concrete structures. According to Tuutti's model (Tuutti 1982), the service life of a reinforced concrete structure can be divided, from the perspective of reinforcement corrosion, into two periods of time: initiation and propagation, which is graphically illustrated in Fig. 2.2. The initiation period is considered to be the time required by which external agents may penetrate into the concrete and cause the depassivation of the reinforcing steel, whereas the propagation period is characterized by active corrosion, with associated iron dissolution in the anodic regions.

The most common depassivating substances causing corrosion of reinforcement are: (i) the carbon dioxide present in the atmosphere, which decreases the alkalinity of the pore solution of the concrete leading to the dissolution of the passive layer; and (ii) the chlorides from marine environments or de-icing salts, which tend to cause a localized breakdown of the passive film, provided enough water and oxygen are available at the reinforcement.

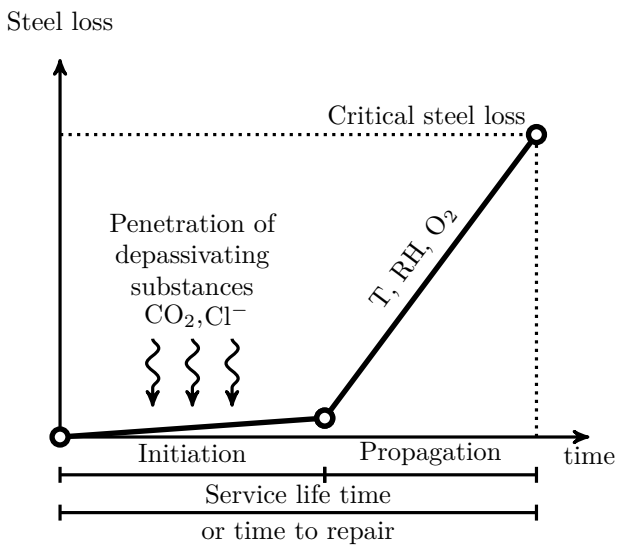

Figure 2.2: *Tutti's model for reinforcement corrosion, modified from (Tuutti 1982)*

When chlorides cause a local breakdown of the passive layer, a pit is typically formed. Hence the term used to describe this type of corrosion is *pitting corrosion*. After pitting has initiated, the environment inside the pit becomes particularly aggressive. This phenomenon is partly due to an increased chloride content in the pit resulting from the migration of chloride ions from the cathodic regions, but also because of the local acidification of the environment caused by the hydrolysis of corrosion products inside the pit. Conversely, the removal of chloride ions from the cathodic areas and the production of hydroxyl ions resulting from the cathodic reaction of oxygen reduction, both tend to strengthen the protective film in the passive regions. Thus, the anodic and cathodic reactions are stabilized and the corrosion process can be sustained (Bardal 2004). The overall process of chloride induced pitting corrosion in concrete can be schematically represented as shown in Fig. 2.3.

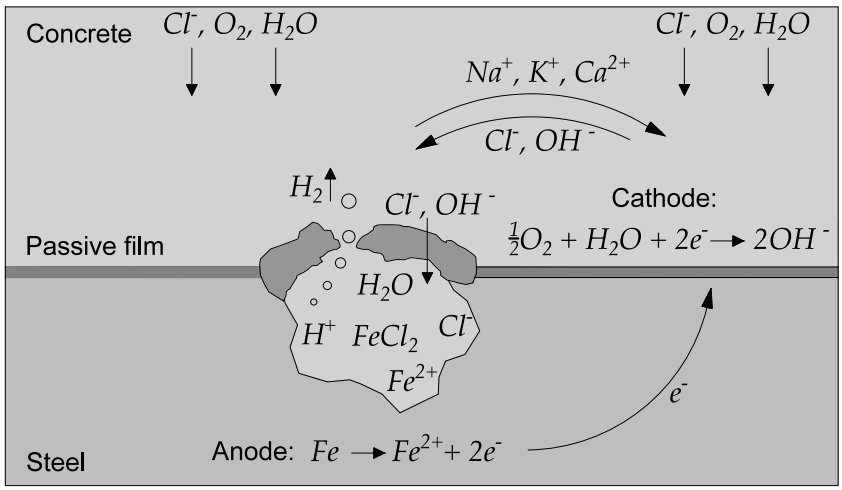

Figure 2.3: *Schematic representation of chloride induced pitting corrosion*

The continuous dissolution of steel tends to decrease the cross-sectional area of the rebar. The ferrous ions released may combine with the hydroxyl ions in the solution to form solid products. These products are insoluble and often present a larger volume than that of the corresponding steel loss. The products are usually deposited on the rebar surface, in the surroundings of the anodic region, filling the pores adjacent to the interface between the concrete and the reinforcement bar (Michel et al. 2011). The gradual accumulation of expansive corrosion products induces inner tensile stresses causing cracking and spalling of the concrete cover and a reduction of the bond between steel and concrete. Both the loss of the rebar section and steel-concrete bond lead to a decrease in structural safety.

2.2 Influence of cracking on corrosion

The phenomena causing degradation of reinforcement in concrete structures are largely dependent on the mechanisms that allow the ingress of water, oxygen and detrimental agents, such as chloride ions or CO_2, as well as mechanisms that allow the transfer of electrical current, to mention a few. The transport mechanisms in concrete can be roughly divided into transport in the bulk material vs. transport in micro- and macro-cracks. Transport in the bulk material can be further classified into four basic mechanisms: *capillary suction* caused by capillary forces, sometimes also referred to as *absorption*; *permeation* driven by a pressure gradient; *diffusion* driven by a concentration gradient; and *migration* due to the presence of an electrical field (Bertolini et al. 2004).

In sound concrete, the concrete cover acts as a physical barrier against the ingress of corrosion-inducing agents. Therefore, the cover depth and quality of concrete are the most important factors influencing the corrosion process of reinforcement. In practice, however, cracks originating from shrinkage, thermal gradients and/or mechanical loading can be found in the vast majority of reinforced concrete structures. These cracks often become preferential paths for the ingress of external agents. As a result, the transport properties of concrete are significantly altered and the durability of concrete structures is negatively affected.

The effect of cracking on the corrosion of reinforcement has been dealt with by several authors in the past (Beeby 1978; Andrade et al. 2010; Vidal et al. 2004; Schiessl and Raupach 1997). Whereas it is generally accepted that the initiation period for cracked concrete is reduced compared to sound concrete, the influence of the crack width on corrosion is still a subject of contemporary study. Although most observations indicate that wider cracks tend to hasten the corrosion initiation, researchers are still debating whether the surface crack width influences the corrosion rate during the propagation period.

Further investigations suggest that other crack parameters might be also relevant to understand the influence of cracks on the corrosion process. Schiessl and Raupach (Schiessl and Raupach 1997) observed that in cracked concrete the preferred corrosion mechanism is macro-cell corrosion, where the anodic site is located at the intersection between the crack and the rebar and the cathodic areas are located along the rebar embedded in sound concrete, as opposed to microcell corrosion, whereby small, neighbouring cathodic and anodic areas coexist in the vicinity of the crack. Under macro-cell corrosion, it is argued the crack spacing or crack frequency might have a significant influence on the corrosion rate due to variations in the anode-to-cathode ratio (Arya and Ofori-Darko 1996). The orientation of the crack with respect to the reinforcement (Poursaee and C. M. Hansson 2008), the self-healing properties of the crack (Edvardsen 1999) or the stress level at the reinforcement (Yoon et al. 2000) have been identified as potentially influencing parameters.

More recently, Pease (Pease 2010) proposed in his thesis the hypothesis that debonding along the concrete-reinforcement interface might be more important for the corrosion of reinforcement than surface crack width. In another thesis, Silva (Silva 2013) concluded

that the steel surface and presence of air-voids at the concrete-steel interface were major factors influencing the development of potential gradients along the rebar surface, thus influencing the corrosion process negatively.

In fact, the only consensus amongst researchers today is that, if the cracks are above a certain limit, i.e. are too large, they will have a negative impact on the durability of RC structures. As a result, as a way to try to obtain durable structures, current structural codes specify permissible crack widths at the surface based on exposure conditions and expected service life.

2.3 Fibre reinforced concrete

The tensile behaviour of cementitious materials may be classified, according to Naaman and Reinhardt (Naaman and Reinhardt 2006), as either strain softening (a quasi-brittle material) or pseudo-strain hardening. Plain concrete is a strain softening material characterized by a sudden loss of stress once the tensile strength of the material has been reached. Conversely, cementitious materials presenting pseudo-strain hardening behaviour exhibit multiple-cracking up to the post-cracking strength, which is higher than the cracking strength. Typical curves for various cementitious materials presenting different tensile behaviour are presented in Fig. 2.4.

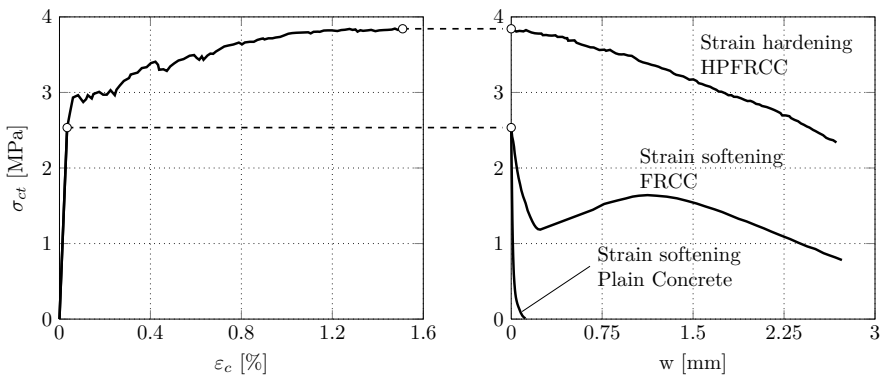

Figure 2.4: *Tensile strength classification of cementitious materials, from (Fantilli et al. 2007)*

Fibre reinforced concrete (FRC) is a cement based composite material reinforced with short, discontinuous fibres which are usually added to the concrete during the mixing process. Fibres are, in general, uniformly distributed and randomly oriented throughout the concrete matrix. The main purpose behind adding fibres to concrete is to better control the fracture process by bridging discrete cracks. As a result, the presence of fibres increases the fracture energy of concrete, enhancing its toughness and leading to a more ductile behaviour. However, the post-cracking behaviour of FRC largely depends on the type and amount of fibres used (Li and Leung 1992). In practice, it is generally

accepted that low fibre contents, below 1%, will lead to strain softening behaviour while pseudo-strain hardening is associated with higher fibre fractions, usally above 2%.

According to Bentur and Mindess (Bentur and Mindess 2007), it is unlikely that fibres will completely replace the conventional reinforcement in structural applications. Nevertheless, fibre reinforcement can carry part of the tensile load through the cracks, thereby alleviating load demands on conventional reinforcement. It has also been observed that the fibres can improve the confinement and thereby the bond behaviour between the concrete and the bars (Jansson et al. 2012). Therefore, a combination of both types of reinforcement could be used to enhance the structural behaviour of RC structures (Blanco 2013). Furthermore, fibre reinforcement could be used together with conventional steel bars for crack control purposes in order to improve the overall durability of a structure (di Prisco et al. 2009).

Among the different materials used to manufacture fibres, steel is often preferred for crack control purposes due its high elastic modulus and good resistance to the highly alkaline conditions of concrete. Nevertheless, the principles governing the corrosion of conventional reinforcement are equally applicable to steel fibres and thus, the risk exists that fibres will corrode in the presence of chlorides. However, it has been reported that compared to conventional rebar steel fibres possess an enhanced resistance to corrosion (Janotka et al. 1989; Sadeghi-pouya et al. 2013). According to Dauberschmidt (Dauberschmidt 2006), this resistance can be attributed to a combination of factors: a) the short length of the fibres, which impedes large potential differences along the fibre and thus limits the formation of distinct anode and cathode regions; and b) the formation of a thin well-defined interfacial layer rich in $Ca(OH)_2$ between the matrix and the fibre with less defects at the interface than conventional reinforcement as a result of the casting conditions (floating in the matrix as opposed to rebar).

However, owing to the limited research and experience available, the use of steel fibres raises questions as to when they are used in combination with conventional reinforcement in chloride environments. Some of these questions are related to the influence that fibres may have with respect to chloride ingress and moisture transport. But the main issues that have yet to be dealt with are the potential risk of galvanic corrosion due to the different steel types used in fibres and traditional reinforcement, and the risk of higher corrosion rates due to lower resistivity of steel-fibre reinforced concrete. In Paper I, these questions are investigated through a review of the existing literature.

3 Overview of Experimental Programme

The experimental programme presented in this study was specifically designed to investigate the influence of fibre reinforcement on chloride-induced corrosion of conventional rebar. The main aspects involved in the corrosion process of reinforcing bars, addressed in this investigation, are: (i) the effect of cracking and crack width; (ii) different loading conditions; (iii) the ingress of chloride; (iv) the electrical resistivity of concrete; and (v) the formation of a galvanic cell between the bars and the steel fibres. In order to study these aspects, the experimental programme has been divided into three types of experiments: long-term corrosion experiments, material tests and galvanic corrosion experiments, all of which are presented in Table 3.1.

The long-term corrosion experiments were aimed at investigating the influence of fibre reinforcement on the chloride-induced corrosion of conventional reinforcement for sound and cracked concrete specimens subjected to different load levels and load history. Using the same mixes as in the long-term corrosion experiments, a series of material tests were carried out. These tests included those aimed at determining the compressive strength and flexural behaviour of the concrete mixes, for mechanical characterization, as well as tests to determine the ingress of chloride and electrical resistivity. A third type of experiment was initiated in parallel to investigate the risk of galvanic corrosion due to differences between the steel used to manufacture conventional reinforcing bars and the steel (or coating) used in fibre technology.

At the present time, the long-term corrosion and the galvanic corrosion experiments are ongoing. Whereas no measurements are being performed on the specimens in the galvanic corrosion experiments, the monitoring of the half-cell potential on the long-term corrosion specimens allowed the determination of the corrosion initiation period for the majority of the specimens studied. Thus, results on corrosion initiation have been included and discussed in this thesis. Furthermore, all material tests included in the experimental programme have already been performed and, therefore, the results obtained are also herein included.

Further results which have not been presented in this thesis include: corrosion rate measurements currently performed using the galvanostatic pulse technique; steel loss estimation of the rebars through gravimetric measurements; analysis of the ratio between the corroded and the total steel surface; and analysis of the pit depth and pit distribution. Additionally, all material tests will be repeated at the end of the experiments to assess the variation of the properties over time.

Table 3.1: Experimental Programme

Long-term corrosion experiments

Stored in fresh water

Loading conditions	Series[a)]	Target crack widths	Number of specimens
uncracked	PL	-	3
	ST	-	3

Cyclic exposure to chloride solution

Load conditions			Series[a)]	Target crack widths	Quantity
uncracked			PL	-	3
			ST	-	3
			HY	-	3
			SY	-	3
cracked	unloaded	1 cycle	PL	0.1, 0.2, 0.3, 0.4	4
			ST	0.1, 0.2, 0.3, 0.4	4
			HY	0.1, 0.2, 0.3, 0.4	4
			SY	0.1, 0.2, 0.3, 0.4	4
		5 cycle	PL	0.1, 0.2, 0.3, 0.4	4
			ST	0.1, 0.2, 0.3, 0.4	4
			HY	0.1, 0.2, 0.3, 0.4	4
	loaded		PL	0.1, 0.2, 0.3, 0.4	4
			ST	0.1, 0.2, 0.3, 0.4	4

[a)] PL=plain ST=steel HY=hybrid SY=synthetic

Material tests

Parameter tested	Specimen type	Dimensions $[mm]$	Specimens per mix
Compressive strength	Cubes	150×150×150	3
Flexural tensile strength	Beams	150×150×550	6
Electrical resistivity	Cylinders	Ø100×50	3
Rapid Chloride Migration Coef.	Cylinders	Ø100×50	3
Bulk Chloride Diffusion Coef.	Cubes	150×150×150	2

Galvanic corrosion experiments

Series	Concrete and fibre type		Fibre content % vol.	Number of specimens
Reference	Plain Concrete		-	3
Type A	SFRC	Low Carbon	0.5	3
			1.0	3
		Zinc Coated	0.5	3
			1.0	3
Type B		Low Carbon	0.5	3
			1.0	3
		Zinc Coated	0.5	-
			1.0	3

4 Long-Term Corrosion Tests

This section provides a detailed description of the long-term corrosion experiments carried out in this project, together with a discussion of the choices made during the planning phase. Fig. 4.1 shows the most relevant parameters considered, divided into four main categories: Specimen characteristics, Fibre reinforcement, Exposure conditions and Loading conditions. A selection of previous experiments carried out by other researchers is included in Section 4.1 to present different possible arrangements that have been used in the past to investigate the corrosion behaviour of reinforcement embedded in cracked concrete.

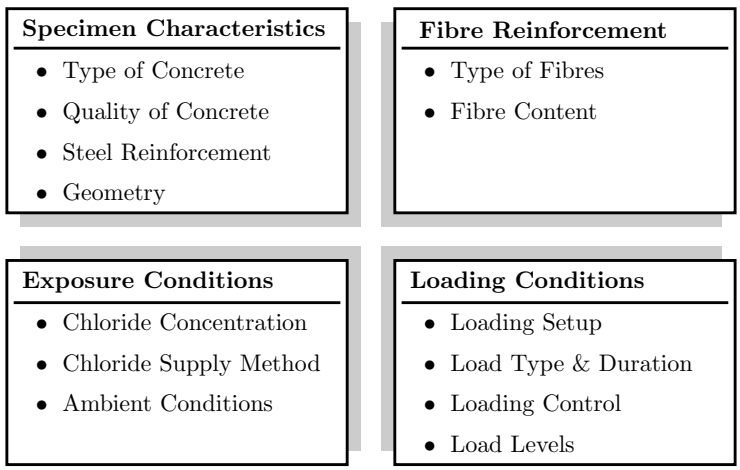

Figure 4.1: *Main parameters considered during the planning phase of the project*

4.1 Experimental work review

Experiments by Arya and Ofori-Darko, 1996

Arya and Ofori-Darko (Arya and Ofori-Darko 1996) investigated the influence of crack space/crack frequency on reinforcement corrosion. In their experiments, the authors used beam elements the geometry and dimensions of which are illustrated in Fig. 4.2. A varying number of equally spaced and parallel sided cracks were formed on each beam by casting shims into the concrete. The depth of the shims was 40 mm and the width was given as a function of the number of cracks in order for accumulated crack width in each beam would total 2.4 mm. The beams were reinforced with a central stainless steel rod and two lateral mild steel rods with a diameter of 8 mm. The beams were stored in a sealed room at a relative humidity of 90% and a temperature of 20 °C for the duration of the experiment. In order to promote corrosion, the beams were periodically sprayed with a 3% NaCl solution, starting 28 days after casting.

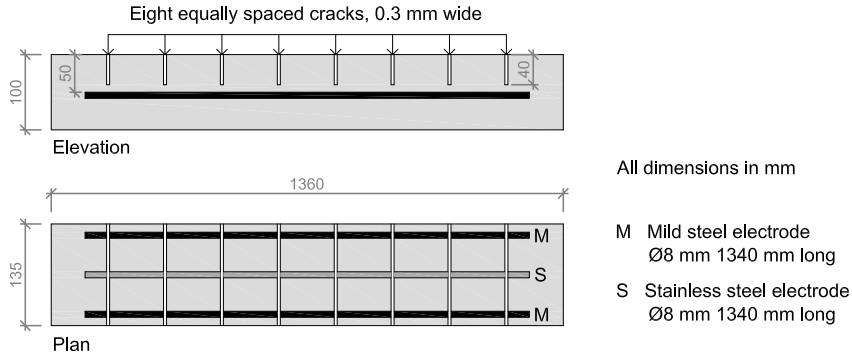

Figure 4.2: *Experimental setup by Arya and Ofori-Darko, from (Arya and Ofori-Darko 1996)*

Experiments by Yoon et al., 2000

The experiments carried out by Yoon et al. (Yoon et al. 2000) aimed at investigating the influence of the load level and sustained load on the corrosion of reinforcement in cracked concrete members. They used a four-point loading configuration to crack concrete beams reinforced with a single Ø19 mm steel bar at 45% and 75% of the ultimate flexural load. Sustained load was applied to the beams using the setup shown in Fig. 4.3. After loading, the specimens were exposed to laboratory environmental conditions with or without 3% NaCl solution ponding at room temperature. They used cyclic ponding consisting of four days of wetting and three days of drying.

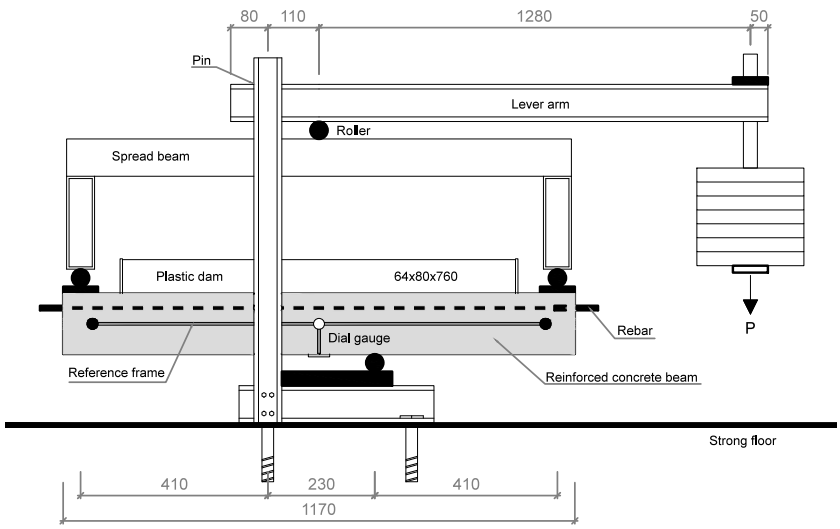

Figure 4.3: *Experimental setup by Yoon et al., from (Yoon et al. 2000)*

Experiments by Vidal et al., 2007

In the experiments reported by Vidal et al. (Vidal et al. 2007), the authors studied the corrosion process of reinforced concrete beams exposed to a salt fog during a period of 17 years. The beams were examined periodically in order to investigate several aspects, including corrosion-induced crack maps, chloride content at the reinforcement level, corrosion distribution along the rebar or mechanical performance. They used real-scale beam elements reinforced with both longitudinal and shear reinforcement as depicted in Fig. 4.4. The beams were subjected to sustained loading, at two different load levels, using a three-point bending configuration and were then stored in a confined room where they were exposed to a salt fog containing 35 g/L of NaCl. The fog was sprayed continuously during the first six years and under weekly cycles during the remainder of the experiment, while the temperature was kept constant at about 20 °C up to nine years and, thereafter, they were subjected to variable temperatures fluctuating between −5 °C and 35 °C.

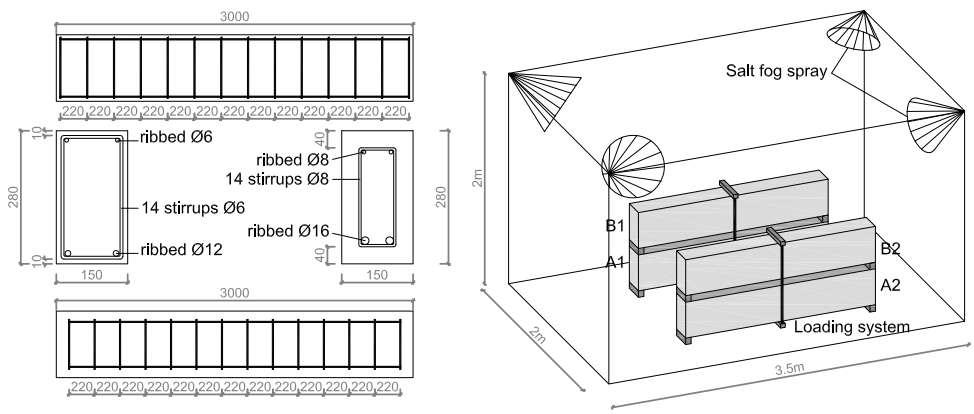

Figure 4.4: *Experimental setup by Vidal et al., from (Vidal et al. 2007)*

Experiments by Jaffer and Hansson, 2008

Jaffer and Hansson (Jaffer and C. Hansson 2008) designed an experimental programme to investigate the influence of dynamic loading on the corrosion of cracked concrete specimens. They used concrete beams reinforced by two Ø11.3 mm carbon steel bars. Some beams were kept undamaged and the remainder were subjected to either static or dynamic loading. Brackets were installed on pairs of beams to apply the load using a three-point bending configuration, as illustrated in Fig. 4.5. Static load was introduced by tightening the nuts on the threaded rods while dynamic load was achieved using an air cylinder and a piston. As for the exposure conditions, the beams were placed upright in containers, partially immersed in a 3% chloride solution and then subjected to cyclic wetting and drying two-week periods.

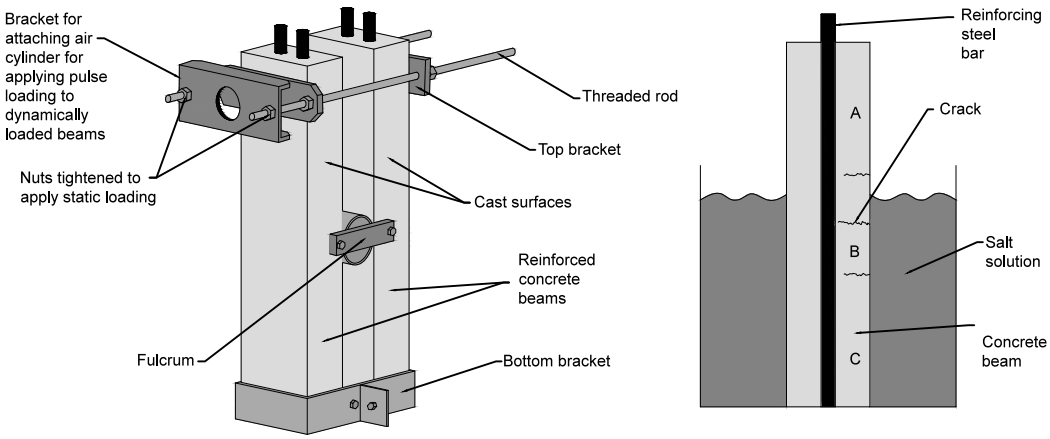

Figure 4.5: *Experimental setup by Jaffer and Hansson, from (Jaffer and C. Hansson 2008)*

Experiments by Tammo, 2009

In his thesis, Tammo (Tammo 2009) studied how different combinations of the concrete cover, crack width and steel stress influenced the initiation of reinforcement corrosion. Concrete beams with varying cover depth, 20, 40 and 60 mm, were reinforced using either two Ø8 mm bars or one Ø12 mm bar. Before casting, the steel bars were mechanically cleaned using a rotating steel brush in order to obtain a uniformly clean surface. After a curing period of 28 days, the beams were cracked under three-point bending and subjected to three different stress levels, 0, 250 and 380 MPa, putting the beams together, two by two, on test rigs. Thereafter, the specimens where moved to a climate room with a constant temperature and relative humidity of 20 °C and 60 %, respectively. Exposure to chlorides was achieved using strips of a special textile material with a high absorption capacity in contact with the cracked surface of the beams and applying salt solution containing 10 % NaCl.

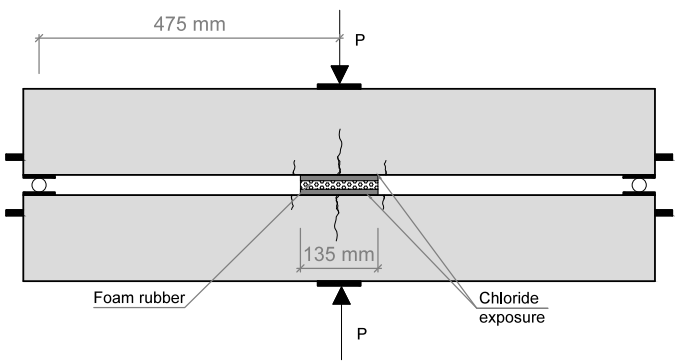

Figure 4.6: *Experimental setup by Tammo, from (Tammo 2009)*

4.2 Discussion of parameters

Planning an experimental programme always involves facing a vast number of choices and decisions. Those decisions will, to a certain extent, determine the results of the experiments and, therefore, need to be thoroughly considered. Based on the desired outcome and available resources, some criteria or requirements need to be established, for example, in terms of cost, duration, etc.

In this project, three characteristics have been identified as highly desirable to shape the development process of the experimental programme. In the first place, the experiments should resemble, as far as possible, the actual conditions to which real structures are subjected to obtain meaningful results. However, real structures are subjected to highly complex conditions that involve a large number of variables. Therefore, experiments should be simplified in order to be able to relate the experimental observations to their causes. Furthermore, the experiments should be carried out within the time frame of the project. Since the initiation period of reinforcement corrosion in concrete structures can take several years, the experiments should be designed to hasten this process to meet pre-established time restrictions.

When more than one criterion is involved, it is often impossible to completely fulfil all criteria simultaneously and thus, it is necessary to compromise. This is illustrated in Fig. 4.7, where the relationship between the three different criteria defined for this project, i.e. realistic conditions, simple setup and accelerated process, is graphically presented.

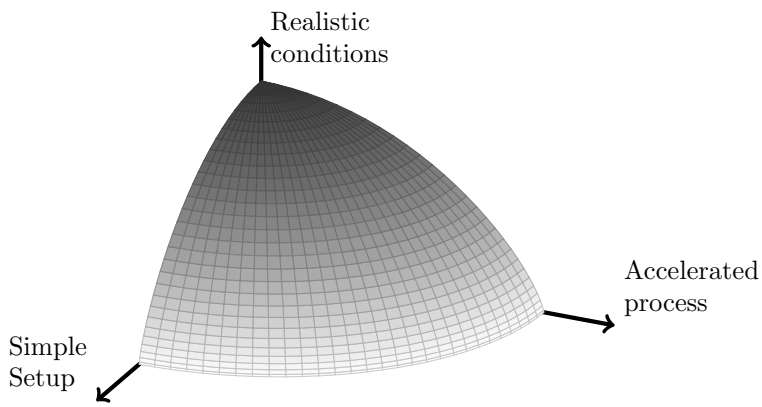

Figure 4.7: *Desired properties of the experimental programme used as criteria for decision-making process*

As already mentioned at the beginning of this chapter, the different parameters defining the experimental project can be classified into four categories. In the following, these categories are presented, enumerating the various parameters and motivating the choices made.

4.2.1 Specimen characteristics

This category involves a large number of choices and, therefore, can be further divided into two subcategories, namely, choices regarding the *materials* as well as choices regarding the *geometry* of the specimens.

Type of concrete

Initially, it was decided that a Self-Compacting Concrete (SCC) mix should be used in this project to compensate for the reduction of workability resulting from the addition of fibres. Despite the fact that SCC is not the main type of concrete used today in civil engineering structures, it is likely that in the near future, its application will spread due to several advantages such as the reduced time for casting, higher quality or better surface finishing of concrete.

Quality of concrete

The quality of concrete is of utmost importance for durability design. The water to cement ratio, w/c, is one of the key parameters. Real structures located in highly aggressive environments are usually cast using very dense concrete mixes with w/c values around of 0.4 or lower. In this case, however, such choice would lead to very long corrosion initiation periods that would most certainly exceed the time frame of the project. On the other hand, current standards provide recommendations on maximum w/c, minimum strength and minimum cement content for concrete, based on the exposure class. Table 4.1 shows an extract from (EN 206-1 2000) for the chloride-induced corrosion exposure classes. As observed, the limitations on the w/c vary between 0.45 and 0.55 in general and between 0.45 and 0.50 for the case of chlorides from the sea. Therefore, an adequate w/c ratio would range from 0.45 to 0.50.

Table 4.1: Recommended limiting values for composition and properties of concrete, from (EN 206-1 2000)

	Exposure class					
	Chloride-induced corrosion					
	Chlorides from sea water			Chlorides other than from sea water		
	XS1	XS2	XS3	XD1	XD2	XD3
Maximum w/c	0.50	0.45	0.45	0.55	0.55	0.45
Minimum strength class	C30/37	C35/45	C35/45	C30/37	C30/37	C35/45
Minimum cement content (kg/m^3)	300	320	340	300	300	320

Steel reinforcement

Regarding the choice of reinforcing steel, the objective was to use the same type and quality of steel as can be found in the construction of current civil engineering structures. Moreover, to emulate realistic conditions of the rebar in concrete, the steel bars were used as received, i.e. no surface treatment was performed prior to casting. However, since the bars presented signs of light rusting, the initial rust content was assessed by comparing the weight of 15 reference samples before and after being mechanically cleaned with a rotating steel brush.

The number of reinforcing bars embedded in each specimen was set to three mainly due to two reasons: (i) to allow for statistical evaluation of the results of each specimen and (ii) to investigate the influence of the relative position of the bars within the concrete element, i.e., center or edge position. Although common bar diameters used in real structural members tend to be large (Ø16, Ø20, Ø25) to decrease the number of bars and keep a wide bar spacing, the bar diameter in this study had to be reduced to ensure tensile failure of the reinforcement while minimizing cross-sectional dimensions.

The addition of shear reinforcement in the form of stirrups was considered during the initial stage of the project but was later discarded because of two major drawbacks: (a) the use of stirrups would imply an increase of the specimen dimensions in order to keep a fixed concrete cover, which would represent a higher self-weight of the specimens, higher load demands and greater storage requirements; (b) stirrups, in contact with longitudinal bars, might promote macro-cell corrosion which would significantly complicate the analysis of results considering the number of variables adopted in these experimental series, including the addition of fibre reinforcement.

Geometry

The main geometrical parameters to be defined were the cross-sectional dimensions, the concrete cover, the bar spacing and the length of the specimens. Similar to the w/c ratio, the concrete cover is known to be fundamental to corrosion protection and, therefore, structural codes recommend large covers, usually above 50 mm for aggressive exposure classes. Despite the fact that the crack limiting effect of fibres would be more noticeable in specimens with larger concrete covers, uncracked specimens would most likely remain uncorroded during the full length of the experiments. Therefore, the convenient depth of the concrete cover should be reduced with respect to the recommended values to hasten the initiation of corrosion but should be large enough to allow the fibres to be placed in the cover and to include the arrested crack effect.

A minimum bar spacing is provided to ensure that the concrete can flow adequately between the reinforcing bars to fill all the corners of the formwork, as well as to guarantee correct bonding between steel and concrete. When using fibre reinforcement, the separation between bars needs to take into account the length of the fibres in order to prevent

their obstruction and ensure a homogeneous distribution throughout the matrix. Based on this reasoning, the bar spacing was chosen as the maximum value resulting from the following: $\varnothing_{bar}$, $\varnothing_{agg}$+5 mm, 20 mm (EN 1992-1-1 Eurocode 2 2004) and $1.25 \times l_{fib}$.

As previously mentioned, the cross-sectional dimensions were optimized to obtain the lightest possible specimen given the already established requirements while promoting a ductile failure mechanism characterized by reinforcement failure in tension under a three-point bending loading setup. Likewise, the length of the specimen was determined to avoid shear or anchorage failure mechanisms.

4.2.2 Fibre reinforcement

Types of fibres

Fibre reinforcement is available in a wide range of materials (metallic, synthetics, glass, natural materials) with the consequent variation of their mechanical properties. Additionally, fibres may differ in length, aspect ratio, cross section, shape and surface finishing. Fig. 4.8 shows a variety of commercially available fibres.

Figure 4.8: *Examples of commercially available fibres*

According to Naaman (Naaman 2003), the desirable properties for fibres to be effective in cementitious matrices are: (1) A significantly greater tensile strength than the matrix; (2) a bond strength comparable to the tensile strength of the matrix or higher;

(3) an elastic modulus in tension higher than that of the matrix; and (4) enough ductility to avoid fibre breakage. Additionally, fibres should present good durability and ought to be able to withstand the high alkalinity of the concrete pore solution.

Given the much higher elastic modulus of steel compared to that of concrete and the good compatibility between both materials, steel fibres were chosen as the primary type of fibre to be investigated. Steel fibres may be susceptible to corrosion and although corrosion resistant steel fibres such as zinc-coated fibres are available, the fibres selected were end-hooked low-carbon steel fibres, as they represent the most widely used type of fibre.

Nevertheless, since corrosion of the fibres and a reduced resistivity of the concrete caused by the conductive nature of steel fibres might influence the overall durability performance of concrete structures negatively, an alternative synthetic fibre type was included in the programme. In this case, PolyVinyl Alcohol (PVA) fibres were the preferred choice due to their reasonably high elastic modulus compared to other synthetic fibres, i.e. in the same order of magnitude as that of the concrete, and a good bond performance due to chemical bonding between the PVA fibres and the cement paste.

A third type of fibre reinforcement was employed using a combination of the aforementioned steel fibres and a short version of the PVA fibres to reinforce concrete at various scale levels. The reason for this choice was that the inclusion micro-fibres that would better control the development of micro-cracks and in particular, bond-stress induced cracks around the reinforcement which are prone to damage the steel-concrete interface and reduce the bond capacity. This step was taken to investigate the hypothesis that interfacial damage or local defects between the concrete and the steel might have a greater impact on corrosion than surface crack width. The three types of fibre are presented in Table 4.2 together with their properties.

Fibre content

Together with the physical properties of the fibres and the bond behaviour between fibres and matrix, the amount of fibres is another factor governing the performance of fibre reinforced cementitious composites. As discussed in Section 2.3, large volume fractions of fibres may lead to pseudo-strain hardening behaviour characterized by multiple cracking and a post-cracking strength greater than the cracking strength. However, in this project the objective has been to utilize fibres in combination with conventional reinforcing bars for crack control, which can be obtained for moderate fibre contents of below 1%. Thus, a relatively low dosage of 0.5% by volume was chosen for the steel fibre mix. The same global dosage was used for the combination of macro-steel fibres and micro-PVA fibres, with partial contents of 0.35% and 0.15%, respectively. However, given the reduced efficiency of macro-PVA fibres caused by their lower modulus of elasticity, the volume fraction for the mix containing this type of fibres was increased by a factor of 1.5, i.e., to 0.75% by volume.

Table 4.2: Fibre reinforcement properties

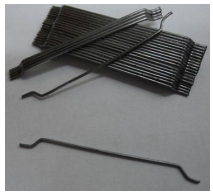

Property	Dramix® 65/35-BN	Kuralon™ RFS400	Kuralon™ RF4000
Material	Low carbon steel	Polyvinyl Alcohol	Polyvinyl Alcohol
Length [mm]	35	18	30
Diameter [μm]	550	200	660
Aspect ratio	65	90	45
Shape	End-hooked	Straight	Straight
Tensile Strength [MPa]	1100	1000	800
Young's Modulus [GPa]	210	30	29

4.2.3 Exposure conditions

In accelerated corrosion tests, it is common practice to add chlorides to concrete during the mixing process or to apply external current to the reinforcement to promote corrosion. However, these methods are not realistic and do not take into consideration the transport mechanism involved in the process of chloride ingress. Therefore, in an attempt to attain realistic results, natural corrosion through the exposure to a highly concentrated salt solution was chosen as the method to trigger corrosion initiation.

Chloride concentration

Once the concrete quality and the cover depth have been determined, the chloride concentration remains the main parameter driving the ingress of chlorides towards reinforcement. In order to estimate the concentration that should be employed, an analytical model, the ClinConc model (Tang 2008), was used to estimate the chloride ingress profiles. Unlike most available models, the ClinConc model only considers the free chlorides in the diffusion equation, thus enabling a relationship between the surface chloride content in the concrete and the chloride content in the environment solution. Assuming that the corrosion of reinforcement would initiate if a critical chloride concentration ranging from 0.4% to 1.0% by weight of cement was reached at the reinforcement level and considering six months as a suitable duration for the initiation period, the chloride ingress profiles were calculated for various initial concentrations. As displayed in Fig. 4.9, for a 30 mm concrete cover, the results showed that a concentration of about 100 g/l in the solution would be adequate to reach the upper limit of the critical chloride content after six months. The input parameters for the ClinConc model used in the analysis are found in Table 4.3.

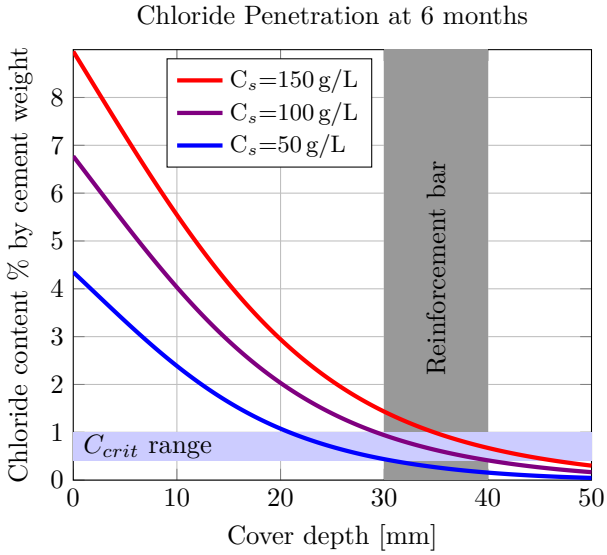

Figure 4.9: *ClinConc model analytical prediction of chloride ingress profiles for 6 months*

Table 4.3: Input parameters for the ClinConc model

w/c [−]	Cement content kg/m^3	Air content %	Porosity %	$[OH]_{6m}$ mol/l
0.47	360	4.0	11.5	0.53*

Diffusivity, D$_{mig}$ $\cdot 10^{-12}$ m^2/s	Time meas. D$_{mig}$ days	Time dependency D [−]	Age exposure days
10	28	$\beta_t = 0.152 \cdot (w/c)^{-0.6}$ *	120

Binding Isotherm Slope	Binding Non-linear exponent	Factor binding time dependency
f_b=3.6*	β_b=0.38*	$f_t = 0.36ln(t_{cl} + 0.5) + 1$*

*Parameters taken from (Tang 2008)

Chloride supply method

As observed in Section 4.1, there are numerous methods by which a source of chlorides for corrosion testing of concrete elements may be provided. Concrete specimens can be subjected to ponding using a saline solution or can be stored in a climate room with salt fog; they can be sprayed with a chloride solution or immersed therein; they can be in contact with a highly permeable textile material soaked in salt water or may even be placed in a natural marine environment. Since no standardised procedure exists for corrosion testing of cracked concrete elements, various ways to supply chlorides were evaluated. Each alternative supply method was evaluated according to five criteria differently weighted by assigning a value ranging from one to three as presented in Table 4.4. The total score of each alternative was calculated as the sum of the individual weighted values. High scores indicate preferred alternatives, hence immersion was chosen as the best way by which chlorides can be supplied.

Table 4.4: Evaluation of chloride supply methods

Criterion	Weight	*Spray*	*Fog chamber*	*Immersion*	*Ponding*	*Natural*
Automatized process	0.15	2	3	2	1	3
Economical cost	0.20	2	1	2	2	3
Control of Cl^- concentration	0.20	2	3	3	3	1
Homogeneous exposure	0.15	2	3	3	1	3
Reduced initiation period	0.30	3	3	3	3	1
	1.00	2.30	2.60	2.65	2.20	2.00

In addition to the chloride supply method used, the exposure procedure, i.e. continuous or cyclic exposure, is important. In concrete elements subjected to cyclic wetting and drying periods, as is the case of tidal and splash zones in marine structures, capillary suction of salt water and subsequent evaporation cause the accumulation of chlorides just above the sea water level, which is illustrated in Fig. 4.10. This mechanism does not only yield a higher concentration of chlorides in the concrete but may also provoke micro-cracks caused by salt crystallisation, thereby providing an additional source of degradation.

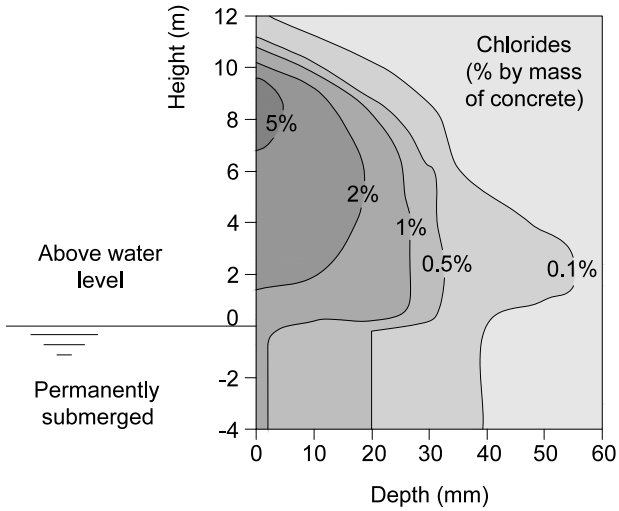

Figure 4.10: *Example of chloride-penetration contours in a marine structure as a function of the height above the sea water, from (Bertolini et al. 2004)*

Ambient conditions

The temperature influences the diffusion of chloride ions and the binding capacity of concrete as well as the electrochemical reactions at the steel/concrete interface and the ionic flow between the anode and the cathode. The humidity and degree of saturation of the concrete, also influence the mobility of the chloride ions as chloride can only be transported dissolved in the concrete pore solution. Therefore, the temperature and humidity can have a significant impact on the corrosion process of reinforcement, both on the initiation and propagation periods. However, a completely controlled climate where temperature and relative humidity are regulated can only be achieved by isolating the specimens from the outside environment, e.g. by a climate room. Given the large number of specimens included in these experiments, this option was discarded. Instead, temperature and relative humidity were continuously monitored at a frequency of one measurement every hour.

4.2.4 Loading conditions

Although a certain number of specimens need to remain undamaged for the sake of comparison, the main purpose of the experiments is to investigate whether fibres, by means of crack control mechanisms, may beneficially influence the corrosion process of reinforcing bars in concrete. Therefore, cracking must be induced; in this study it was chosen to load the specimens as opposed to "cast in" cracks, where the effect of fibre reinforcement could not be accounted for.

Loading setup

Often large amounts of secondary reinforcement are required at locations where high bending moments cause wider cracks. Therefore, in order to induce cracking, specimens should be subjected to loading in bending. Although real structures are subjected to a variety of loads as well as restraint stresses (due to temperature and shrinkage), the most common setups used in practice for laboratory tests are three-point and four-point bending tests.

Whereas a four-point bending scheme provides a region with constant moment where cracks of similar width are expected, in a three-point bending scheme a wider crack is usually located right under the loading point, being easier to monitor. In addition, four-point bending requires higher loads to achieve an equivalent bending moment, thus favouring shear failure compared to three-point bending. Furthermore, when using four-point bending setups, potential contact problems may arise at the load application points, leading to different load values and asymmetrical moment distribution.

Type and duration of the load

Civil engineering structures undergo different types of loading throughout their service life time. The load application time, load duration and load periodicity may vary significantly. Some loads can be considered to be quasi-statically applied and applied remain permanently, e.g. the self-weight, whereas others can be regarded as dynamic loads and be present only during short periods of time. Although it would be interesting to investigate a wide range of different scenarios, this option is outside the scope of this project. Therefore, in these experiments, loads were applied for a short period of time, quasi-statically and only once before the initiation of the corrosion tests to induce cracking. Later some specimens were subjected to sustained loading with a constant load value over the time.

According to the literature, however, two specific factors related to the loading conditions have been regarded as particularly interesting to the corrosion process: the stress level at the reinforcement and the degradation of the interface between steel and concrete. The first factor can be investigated by subjecting specimens to sustained loads while the corrosion tests are carried out. As to the second factor, interfacial degradation increases with increasing load levels but given a certain load limit, such degradation can also be achieved by successive unloading and re-loading.

Loading control and loading levels

For the loading procedure of the specimens, it is necessary to define the end of the test in order to be able to reproduce it with enough accuracy. The end of the test may be associated with such factors as a load threshold or a maximum deflection. Whereas a load threshold can be easily measured and simply to defined, e.g. in relation to the ultimate load, a reduced crack width in FRC specimens would prevent the influence of cracks to be discerned from the influence of fibres on rebar corrosion. Therefore, aiming at the

same surface crack width would presumably equate all specimens in terms of corrosion susceptibility, regardless of the addition of fibres.

If various load levels, or in this case various crack widths, are to be studied, it is important to define realistic boundaries. Despite the fact that structural codes define strict crack width limitations, commonly 0.1 mm at the reinforcement level for highly aggressive environments, existing structures often present wider cracks at the concrete surface. Large cracks of around 1 mm or wider, which have been reported to have a negative impact on both corrosion initiation and corrosion rate are on the other hand unrealistic and, therefore, of little interest. Consequently, cracks slightly wider than the limitations specified in the codes were subjected to study.

4.3 Description

The long-term corrosion experiments comprises 54 beam specimens, six of which were used as reference samples. The other specimens were divided into several groups and subjected to different loading conditions. The loading cases considered included: (1) *Uncracked* series: sound specimens, which were never loaded; (2) *Unloaded* series: cracked specimens which were loaded once and then kept unloaded; (3) *Cyclic* series: cyclically loaded specimens, which were subjected to five load cycles and then kept unloaded, with the intention of causing a higher interfacial damage than (2); and, finally, (4) *Loaded* series: loaded specimens, which were preloaded to induce cracking and then kept loaded with a constant and sustained load, using steel brackets and a hinge.

4.3.1 Specimen design and materials

The geometry of the specimens employed in the present investigation are illustrated in Fig. 4.11. The beams featured total dimensions of 100 × 180 × 1100 mm and were reinforced with three Ø10-ribbed bars. The reinforcement was positioned to obtain a clear concrete cover of 30 mm at the bottom and sides of the beam whereas the distance between bars was kept at 45 mm, approximately 1.25 times the fibre length. Longitudinally, the reinforcement bars also had a concrete cover of 30 mm at one of the ends whereas they stuck out about 50 mm at the other end to allow electrical connections.

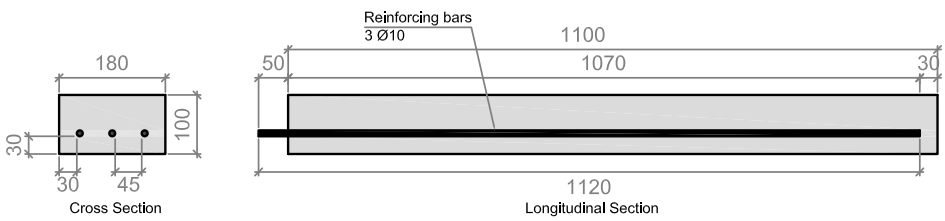

Figure 4.11: *Specimen geometry, measurements in mm*

The same concrete mix, apart from the addition of fibres, was used for all series in this project. Table 4.5 summarizes the concrete mix proportions. The concrete was designed with a w/c ratio of 0.47 and was chosen to be a self-compacting mix to guarantee a good flowability of the concrete despite the addition of fibres. As reinforcement, a grade B500B, steel defined in Eurocode 2 as normal ductility was used. The average values of the yield stress and strain, tensile strength, maximum strain and elastic modulus, obtained through tensile tests performed on 450 mm long bars, were $f_y = 546$ MPa, $\varepsilon_y = 0.269\%$ $f_u = 626$ MPa, $\varepsilon_u = 9.76\%$ and $E_s = 204$ GPa, respectively. Steel bars were used as received, i.e., without applying any surface treatment to them prior to casting. Additionally, all reinforcing bars were weighed before casting for subsequent weight loss assessment.

Table 4.5: Mixture proportions, in kg/m^3

Component				
Cement (CEM I 42.5N SR 3 MH/LA)			360	
Limestone filler (Limus 40)			165	
Fine aggregate (sand 0/4)			770	
Coarse aggregate (crushed 5/16)			833	
Effective water			169	
Superplasticizer - Glenium 51/18			5.76	
Air entrainer - MicroAir 105			0.72	
Fibre (vol.%)	Plain	Steel	Hybrid	Synthetic
Steel - Dramix® 65/35-BN	-	0.5	0.35	-
PVA - Kuralon™ RFS400	-	-	0.15	-
PVA - Kuralon™ RF4000	-	-	-	0.75

Four different series of specimens, hereafter referred to as plain, steel, synthetic and hybrid, were cast using embedded conventional reinforcement. The series differed by the type of fibre reinforcement used, which was: none for the plain series; 35 mm end-hooked steel fibres for the steel series; 30 mm straight PolyVinyl Alcohol (PVA) fibres for the synthetic series; and a blend of the steel fibres mentioned and 18 mm long PVA fibres for the hybrid series. The fibre characteristics have been summarized in Table 4.2.

4.3.2 Casting and curing

During casting of the beam specimens, in order to guarantee the correct positioning of the rebars, fibre-reinforced concrete spacers from MaxFrank® were used. The spacers, designed with a high-density concrete and low chloride diffusion coefficient ($< 5.0 \times 10^{-12}\,\mathrm{m}^2/\mathrm{s}$, had a nominal height of 60 mm to permit positioning them alongside the larger concrete cover to hinder the ingress of chlorides through the interface between the spacers and the cement paste. The beams were cast with the bars hanging from the spacers, as shown in Fig. 4.12, a choice made while bearing in mind that smaller cover layers produce smaller concrete settlements under the reinforcement, thus minimizing the potential

interfacial defects along the rebar. Moreover, this setup of the spacers avoided having fibres sticking out from the surface at the concrete on the side of the smaller concrete cover. All specimens were outfitted with a reference electrode embedded in the concrete to allow the continuous monitoring of corrosion potential (see Fig. 4.12).

Figure 4.12: *A detail of a fibre-reinforced concrete spacer (top-left); an embeddable reference electrode ERE20 (top-centre); insulation of reinforcing bars with hard-foam (top-right); and a general view of the formworks (bottom)*

The beam specimens were cast in plywood formwork and kept covered with a polyethylene sheet for 24 hours. After that, the formwork was removed and the beams wetted and wrapped in geotextile and plastic sheets. Thereafter, all specimens were stored (in the wrapping) at room temperature until they were preloaded for a period ranging between 72 and 82 days.

Figure 4.13: *Storage process of the beam specimens for curing*

4.3.3 Pre-loading procedure

A three-point loading configuration, as shown in Fig. 4.14, was used to introduce a desired bending moment to the beam specimens. The distance between the end supports was 1000 mm, and the load was applied at the mid-span. Loading was performed with a double-effect hydraulic jack with a maximum load capacity of 100 kN. Four linear variable displacement transducers (LVDTs) were placed on the concrete beam, two at the mid-span section at either side of the loading plate, and an additional LVDT at each end-support section.

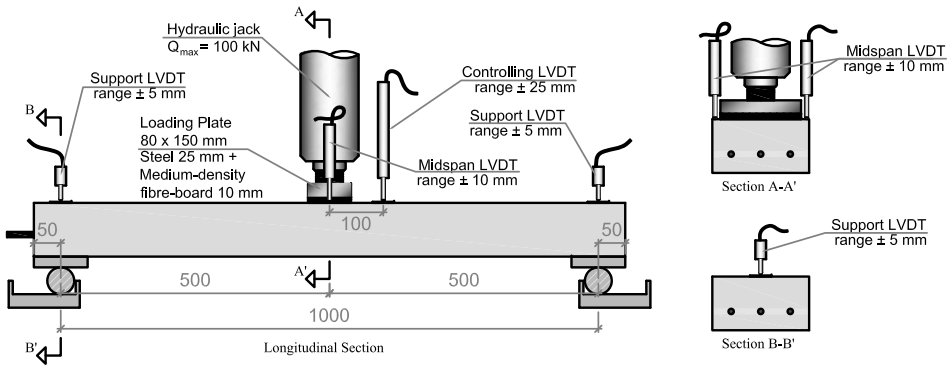

Figure 4.14: *Three point bending setup used during the pre-loading procedure to induce bending cracks, measurements in mm*

Loading was performed by displacement control at a displacement rate of 0.1 mm/min, whereas for the cyclic loaded specimens (subjected to five loading cycles), the displacement rate was 1 mm/min. During the loading procedure, the crack width opening of the widest crack formed in each specimen was measured using a crack detection microscope with a magnification of 20× and an accuracy of 0.02 mm. Table 4.6 shows the maximum applied loads during the pre-loading procedure for all cracked beam specimens. The target crack width openings were 0.1, 0.2, 0.3 and 0.4 mm. Upon unloading, the remaining crack width openings generally ranged from 0.02 mm to 0.06 mm.

4.3.4 Sustained loading set-up

A sustained load was applied to eight of the specimens using a similar setup as the one described by Jaffer and Hansson (Jaffer and C. Hansson 2008). The beams selected, belonging to the plain and steel series, were coupled into pairs according to the crack width opening aimed during the pre-loading procedure. Stainless steel brackets, consisting of two hollow rollers clamped to the concrete beams using threaded rods and nuts, were installed on the coupled beams about 22 weeks after casting. The specimens were subjected to three-point bending using the set-up illustrated in Fig. 4.15

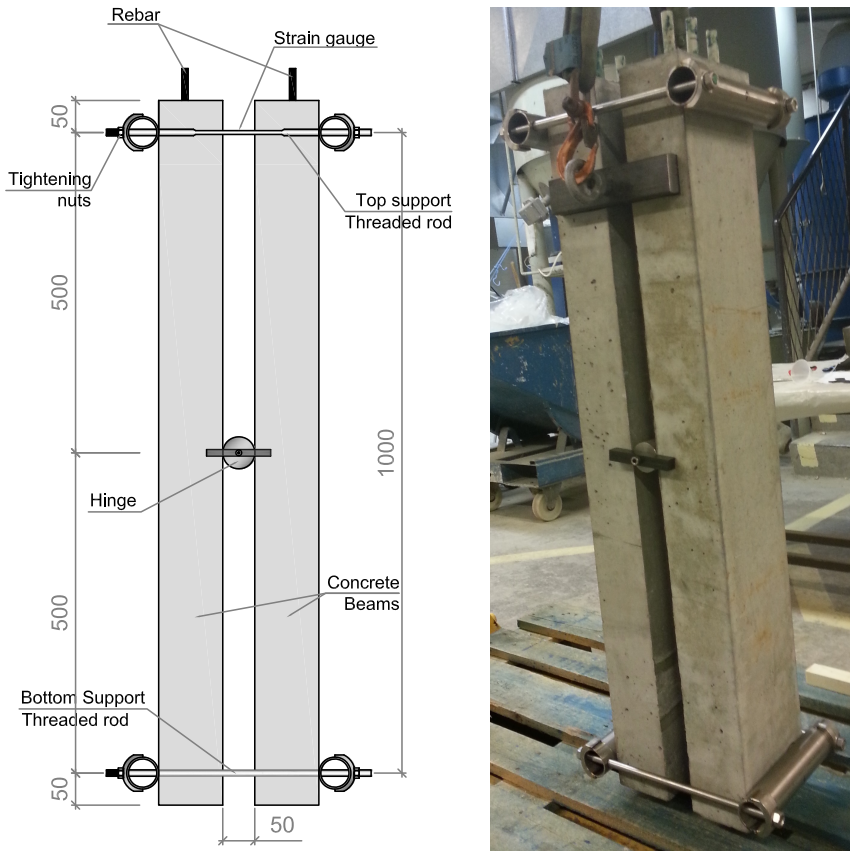

Figure 4.15: *Setup for sustained loading, measurements in mm*

Table 4.6: Maximum applied load during pre-loading procedure for cracked beam specimens, in kN.

		Target crack width [mm]			
		0.1	0.2	0.3	0.4
Plain	Unloaded	12.4	18.5	21.5	27.5
	Loaded	11.5	14.7	27.0	27.5
	Cyclic	14.0	17.0	24.6	25.1
Steel	Unloaded	14.0	21.2	28.6	34.8
	Loaded	16.8	21.5	29.0	33.0
	Cyclic	13.0	24.2	25.6	34.0
Hybrid	Unloaded	13.0	18.3	26.3	33.6
	Cyclic	13.8	22.0	27.0	33.0
Synthetic	Unloaded	12.5	20.2	27.1	31.0

Table 4.7: Applied loads during pre-loading procedure and intended loads for sustained loads, in kN.

	Target crack width [mm]			
	0.1	0.2	0.3	0.4
Plain series				
Max. load reached during pre-loading	11.5	14.7	27.0	27.5
Steel series				
Max. load reached during pre-loading	16.8	21.5	29.0	33.0
Intended load for coupled beams	14.2	18.1	28.0	30.3

The load was introduced by tightening the nuts on the threaded rods. Additionally, strain gauges were placed on the threaded rods of every upper bracket and were calibrated before the beams had been loaded. That was done to accurately measure the load applied during the loading procedure as well as to keep track of the load losses due to creep and relaxation in order to compensate for them. The beams from the plain series were coupled with the beams in the steel series according to target crack width. Since the load applied during the pre-loading procedure had varied for beams belonging to different series, the coupled beams were loaded to an average value as shown in Table 4.7. Consequently, the crack widths for the coupled beams were expected to deviate slightly from target crack widths.

4.3.5 Exposure conditions

After curing and pre-loading, all specimens were kept in laboratory environmental conditions. Before exposing the specimens to chlorides, they were placed standing vertically into plastic tanks and left to soak in potable water during two weeks to ensure that they were saturated prior to chloride exposure. During that period, the 16.5% NaCl solution (corresponding to 10g of Cl^-/100g of solution) was prepared in different tanks.

The exposure of the beams to the chloride solution was performed by partial immersion as shown in Fig. 4.16, setting the water level to submerge 75% of the beam length. The exposure of the beams to chlorides was performed progressively according to their loading conditions; thus, the age of the specimens at the initiation of the exposure was: 18 weeks for the uncracked beams; 20 weeks for the unloaded and cyclically loaded beams; and 22 weeks for the loaded beams.

Figure 4.16: *Beams subjected to partial immersion in 10 % chloride solution*

Immersion was performed cyclically to hasten the corrosion process and to correspond to the XS 3 or XD 3 exposure class in EN 206 (EN 206-1 2000). The cyclic periods consisted of two weeks of wetting, during which the tanks were covered with plastic sheets to prevent evaporation of water, followed by two weeks of drying at laboratory conditions.

The environmental conditions in the laboratory, i.e. temperature and relative humidity, were monitored and recorded hourly during the whole experiment duration using the Vaisala HUMICAP® humidity and temperature probe HMP110 displayed in Fig. 4.17, which averaged 20.5 ± 3.6°C and 45 ± 15%RH, respectively. The chloride content of the solution in the tanks was also measured periodically using test sticks from Quantab® to balance the variation of concentration.

Figure 4.17: *Chloride test sticks from Quantab® (left) and HUMICAP humidity and temperature probe HMP110® from Vaisala (right)*

4.3.6 Corrosion measurements

Half-Cell Potential (HCP)

HCP is an indicator of the thermodynamic state of a metallic surface, which is measured as the potential difference (voltage) between the metal surface and a reference electrode. Commonly used reference electrodes include Saturated Calomel Electrode (SCE), Silver/Silver Chloride Electrode (SSC) or Copper/Copper Sulfate Electrode (CSE) (Pawlick et al. 1998).

In this investigation, the Embeddable Reference Electrode ERE 20 from FORCE Technology was used. The ERE 20 reference electrode is a true reference electrode based on the reaction between MnO_2 and Mn_2O_3 in a highly alkaline electrolyte (pH=13.5). The solution is placed in a stainless steel case to provide electrical contact and the electrode is equipped with an ion-membrane of cement mortar at the tip to ensure good affinity with concrete. Fig. 4.18 shows the ERE 20 reference electrode components. Embeddable electrodes offer the advantage that they can be placed relatively close to the reinforcement, thus reducing errors related to the resistivity of the concrete. Embeddable electrodes, unlike the portable ones, can however only measure the corrosion potential in the vicinity of the electrode location.

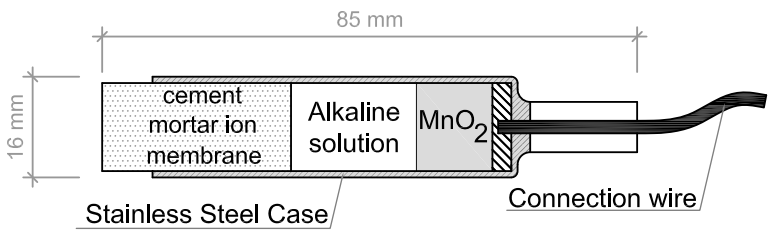

Figure 4.18: *ERE20 - cross section.*

The ERE20 probe, with a diameter of 16 mm and a total length of 85 mm, was placed at 25 cm from the end of the beam where the reinforcement stuck out, with its tip located between two reinforcement bars (see Fig. 4.12). Each electrode was connected to two different ports of a data logger and the circuit was closed using two wires to connect the respective reinforcing bars to the right port, as illustrated in Fig. 4.19. Half-cell potentials were read every five minutes and the hourly average was recorded.

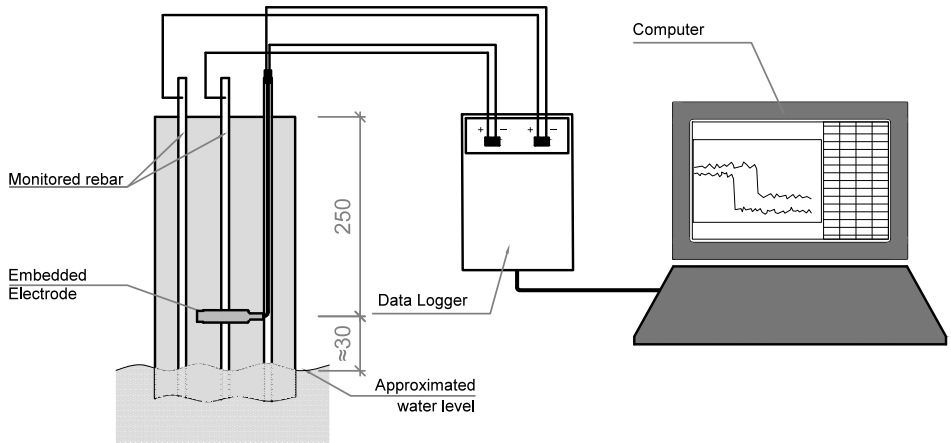

Figure 4.19: *Electrical connection scheme between the electrode, the logger and the rebar*

It is important to note that HCP only describes the thermodynamic state of the metal surface, i.e., it does not by itself provide information about the corrosion rate (current) in the specimens, which is governed by corrosion kinetics. However, HCP can indicate whether the reinforcement is actively corroding or is in a passive state and it may suggest a range of corrosion rates. Table 4.8 shows the probability of corrosion of reinforcement related to the HCP, also called Open Circuit Potential (OCP), for most common reference electrodes.

Table 4.8: Criteria for interpretation of half-cell potentials, according to ASTM C876-09

Open circuit potential (OPC) values [mV]				Risk of
(*vs.* $Cu/CuSO_4$)	(*vs.* CSE)	(*vs.* MnO_2)	(*vs.* SSC)	corrosion
>-125	>-200	>-285	>-95	Low (<10%)
-125 to -276	-200 to -350	-285 to -336	-95 to -245	Intermediate
<-276	<-350	<-336	<-245	High (>90%)
<-426	<-500	<-586	<-395	Severe

Galvanostatic pulse technique

The galvanostatic pulse technique is a rapid non-destructive polarization technique considering the time-dependent behaviour of steel polarization. This technique has been used to evaluate reinforcement corrosion both in laboratory and on site.

A counter electrode placed on the concrete surface impresses, galvanostatically, a brief anodic current to the reinforcement. The applied current, usually in the range of 10 to 200 µA, has a typical pulse duration of between 5 and 10 seconds. The small anodic current results in a change of reinforcement potential, which is recorded by a reference electrode as a function of polarization time. The usual transient response of polarization is shown in Fig. 4.20. Assuming that the transient behaviour of steel polarization can be described by a simple Randles circuit, the polarized potential of reinforcement, V_t, at a given time t can be described by Eq. (4.1) as (Elsener et al. 1997):

$$V_t(t) = I_{app}\left[R_p\left(1 - e^{t/R_pC_{dl}}\right) + R_\Omega\right] \tag{4.1}$$

where R_p is the polarization resistance, C_{dl} is a double layer capacitance and R_Ω is the ohmic resistance. By means of mathematical analysis, i.e. curve fitting and extrapolation of time towards infinity, the ohmic resistance of the concrete and the polarization resistance R_p can be calculated.

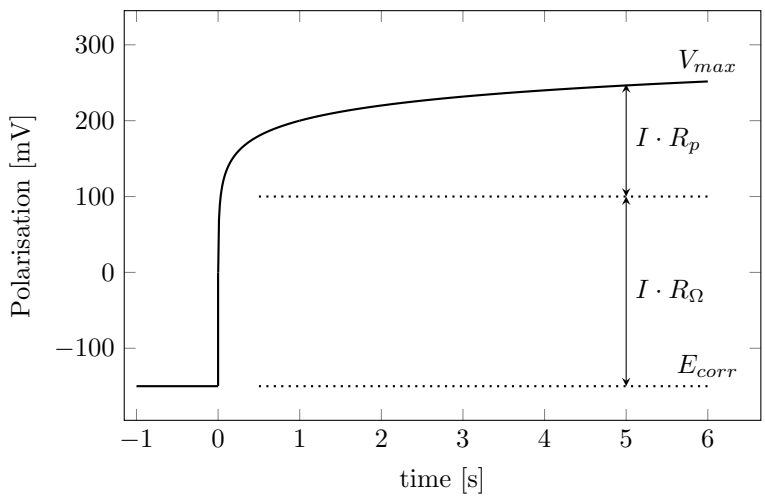

Figure 4.20: *Typical Potential vs time curve as a response to a galvanostatic pulse, after (Song and Saraswathy 2007)*

In the present investigation a handheld instrument, called RapiCor, was used. The RapiCor, developed by Tang (Tang, Fu, et al. 2010), is based on the galvanostatic pulse technique and has been designed for application in real structures. In the RapiCor instrument in Fig. 4.21, all electrodes are located in a handheld, rectangularly shaped

handle measuring 15cm long and 3×4 cm in cross-section. The reference Ag/AgCl electrode (RE) is placed at the centre of the handle. Positioned on either side of the reference electrode are the counter electrodes (CE). A second set of concentric electrodes, the guarding electrodes (GE), is used to confine the current and help to supply a homogeneous current density over a length L_p.

Figure 4.21: *RapiCor handheld device*

The special feature of the RapiCor is that, based on numerical 2D FEM modelling of the current distribution, the effective polarization current Ip is obtained by integrating the current distribution curve through the specified polarization length L_p. The working principle of the RapiCor is presented in Fig. 4.22.

In order to obtain the corrosion rate, X_{corr} (in dimensions of μm/year), from a polarization measurement, the RapiCor device uses Eq. (4.2) (Tang, Fu, et al. 2010):

$$X_{corr} = \frac{BM}{\rho z F} \cdot \frac{I_p}{A \cdot \Delta E_p} \tag{4.2}$$

where,

B : Stern-Geary constant, often assumed as 26 mV,
M : molecular weight of the metal (M=56 g mol^{-1} for Fe),
ρ : specific density of metal (ρ=7.85 g cm^{-3} for Fe),
z : number of ionic charges (z=2 for Fe),
F : Faraday constant (F=96 480 C mol^{-1}),
I_p : polarization current, in µA,
A : polarization area, in cm^2, and
ΔE_p : polarization potential, in mV.

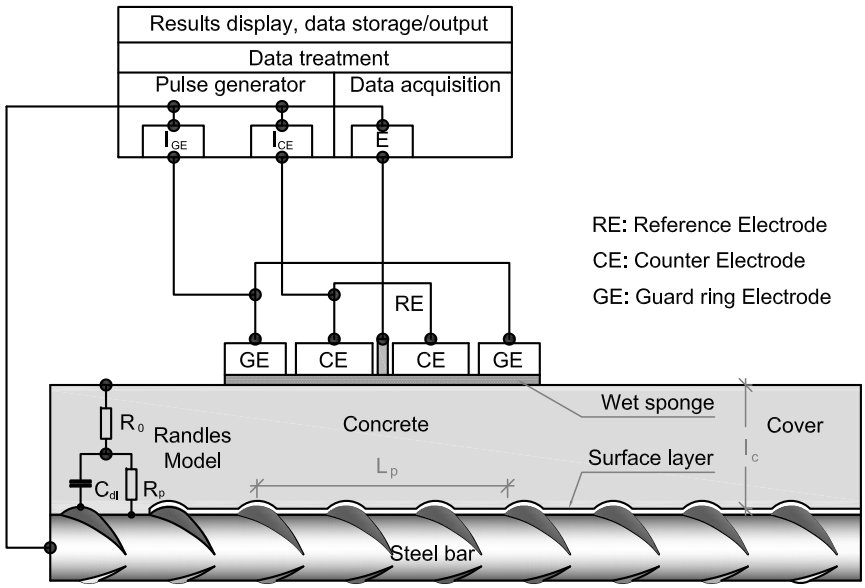

Figure 4.22: *Measurement principle of the RapiCor device, after (Tang, Fu, et al. 2010)*

5 Material Tests

The long-term corrosion experiments constitute the main part of the experimental programme, where the influence of the selected variables on the corrosion process of steel reinforcement bars is investigated. However, as previously mentioned, the corrosion of reinforcement involves a number of different mechanisms. It is important to study those mechanisms individually to achieve a better understanding of the overall corrosion process as well as to identify the factors that might have a greater impact on the results.

Therefore, in order to compare the mechanical, transport and electrical properties of the different mixes used in the long-term experiments, a complementary set of companion specimens were simultaneously cast for material characterization of the different concrete mixes. Table 5.1 shows the material tests carried out in this experimental programme, which are further described in the following text.

Table 5.1: Material tests carried out within the experimental programme

Material tests

Parameter tested	Standard	Specimen type	Dimensions $[mm]$	Specimens per mix
Compressive strength	EN 12390-3	Cubes	150×150×150	3
Flexural tensile strength	EN 14651	Beams	150×150×550	6
Electrical resistivity	[–]	Cylinders	Ø100×50	3
Rapid Chloride Migration Coefficient	NT Build 492	Cylinders	Ø100×50	3
Bulk Chloride Diffusion Coefficient	NT Build 443*	Cubes	150×150×150	2

*Modified testing procedure

5.1 Compressive strength

The compressive strength of each concrete mix was determined using three cubic specimens with a side length of 150 mm. The specimens were cured in water according to (EN 12390-2 2009) and tested under monotonic load after a period of 28 days according to (EN 12390-3 2009).

5.2 Flexural tensile strength

In order to characterize the flexural behaviour of reinforced concrete mixes, i.e. the flexural stress and post-cracking flexural capacity, three-point bending tests (3PBT) according to (EN 14651 2007) were carried out. Beam specimens with dimensions $150 \times 150 \times 550$ mm were cast at the same time as the main beam specimen and were wrapped in geotextile and plastic sheets for a period of 19 weeks. Prior to testing, the beams had been notched and placed into water for 48 hours. Fig. 5.1 shows the loading scheme of the test, together with the measurement equipment used.

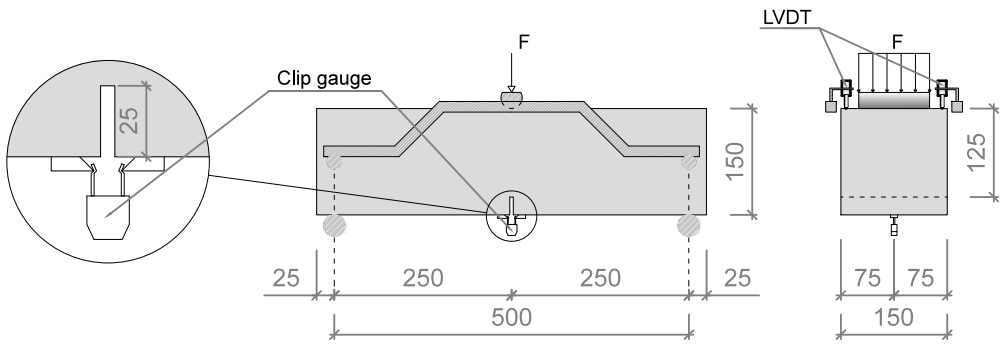

Figure 5.1: *Three-point bending test configuration for determination of flexural tensile strength*

5.3 Electrical resistivity

Electrical resistivity is regarded in the literature as a fundamental parameter to describe the corrosion rate of reinforcing bars in concrete structures, which is often considered to be the limiting factor in aerated concrete members. In this investigation, the electrical resistivity of concrete was assessed as described in (Tang, Nilsson, et al. 2012) using a uniaxial electrode configuration (see Fig. 5.2). The specimens used were $Ø100 \times 50$ mm discs cut out from the central part of larger cylinders with $Ø100 \times 200$ dimensions, which had been cured in water for a period of seven weeks. The discs had been pre-conditioned by being subjected to a vacuum for three hours and had then been immersed in $Ca(OH)_2$ saturated solution for 18 hours. The discs were later positioned between two plate-shaped electrodes and a constant alternating current at 1 kHz was applied. The electrical resistance was measured using an LCR meter after which the resistivity was determined as a function of the specimen geometry according to:

$$\rho = \frac{A}{l} \cdot R \tag{5.1}$$

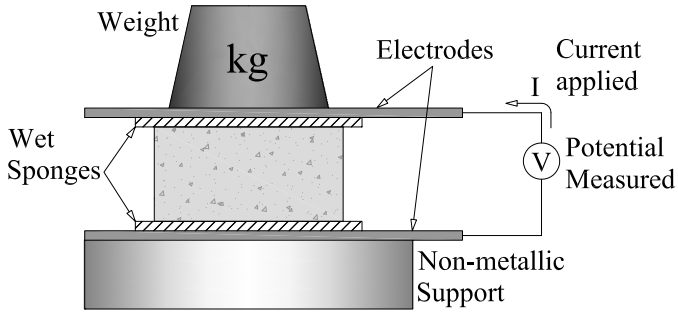

Figure 5.2: *Electrical resistivity test configuration*

5.4 Chloride diffusion coefficient

Despite the fact that in most cases chloride ingress involves more than one transport mechanism, diffusion is considered as the principal mechanism when the moisture condition in the pore system of the concrete remains stable. Furthermore, most of the available models used to predict chloride ingress into concrete rely on the diffusion coefficient of the concrete. Therefore, it is of interest to determine the characteristics of the different mixes in terms of chloride diffusion. To that end, two distinct approaches were adopted: a) determination of the chloride diffusion coefficient from non-steady state migration tests according to (NT Build 492 1999); and b) determination of the chloride diffusion coefficient from long-term bulk diffusion tests according to the (NT Build 443 1995) principle.

The time required to perform migration tests is substantially shorter than for common diffusion tests. This difference is mainly attributed to the fact that in diffusion tests the ionic flow is due to a concentration gradient, whereas in migration test the main driving force is the externally applied electric field. Therefore, it might be questioned whether the results obtained from migration tests are meaningful in terms of describing the diffusion process of chlorides in concrete, especially in the case of concrete reinforced with metallic fibres where the current flow may be significantly altered. Nevertheless, it can be interesting to assess and compare the non-steady state migration coefficient of the different mixes and examine the potential the influence of fibre reinforcement.

5.4.1 Non-steady state migration test

After performing the resistivity tests, the same specimens were fit into a rubber sleeve, ensuring that the contact between the concrete and the rubber sleeve would be water tight to avoid any leakage. The specimens were placed into a plastic box and the catholyte and anolyte were poured into the plastic box and rubber sleeve, respectively. Two plate-shaped electrodes were positioned at either side of the disc as shown in Fig. 5.3, and a constant voltage was applied for 24 hours. After that, the specimens were cut open into two halves and sprayed with a 0.1M silver nitrate ($AgNO_3$) solution to measure the penetration front of chlorides.

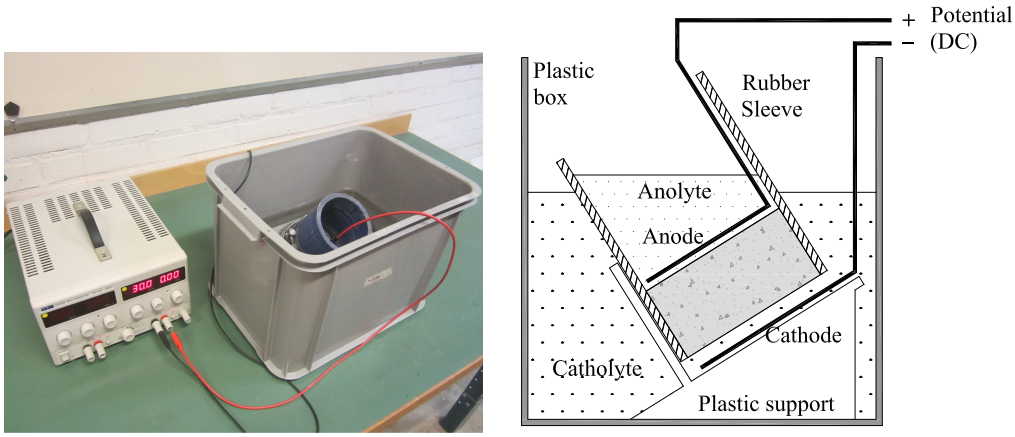

Figure 5.3: *Non-steady state migration test setup*

5.4.2 Bulk diffusion test

Cubic specimens with 150 × 150 × 150 mm dimensions that were cast at the same time as the specimens in the long-term corrosion test were introduced in a plastic tank after a curing period of 30 weeks wrapped in plastic sheets. The specimens were considered to be sufficiently large for the zone from which the powder samples were to be ground to remain unaffected by two and three dimensional ingress of chloride ions during the immersion period. Therefore, the lateral faces of the cubes were not coated. The age of the specimens was seven months when the test was started. Prior to the exposure to chlorides, the specimens were immersed for a week in tap water to reduce the ingress of chloride ions due to adsorption. Thereafter, 10% chloride solution by mass (165g of NaCl by 1000g of solution) was poured into the tank while setting the solution level so there would be at least 50 mm between the top face of the cubes and the free water surface. This procedure led to a ratio of the exposed area of the specimen to the volume of exposure solution of about 7.5 mL chloride solution per square centimetre of exposed surface.

After seven months of immersion, cubes were removed from the tank and Ø75 mm cores were drilled from the centre of the cubes. The cylindrical cores were stored in plastic bags before they were ground to prevent moisture evaporation and the consequent movement of ions towards the surface. Once all the cores had been obtained, powder samples from various depths were collected by grinding the concrete surface, as displayed in Fig. 5.4. The samples collected were then oven-dried at a temperature of 105°C and remained in this condition for two weeks, until they were sent to Cementa Research to have the samples analysed for chloride content according to (EN 14629 2007).

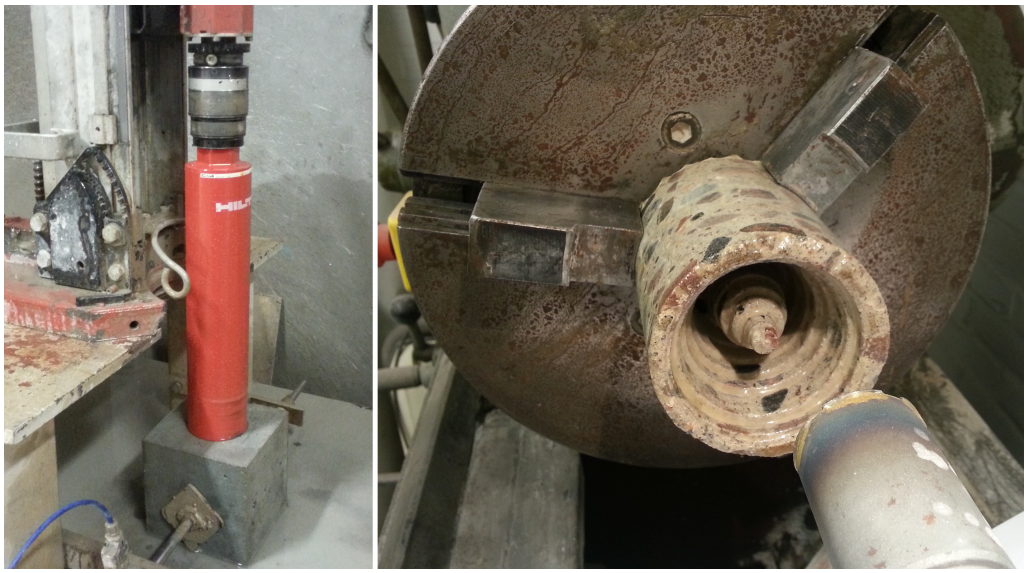

Figure 5.4: *Drilling and grinding process to obtain powder samples from the bulk diffusion test specimens*

6 Galvanic Corrosion Tests

In situations where two dissimilar metals or alloys are electrically connected at the same time as they are in contact with a solution that can act as electrolyte, a galvanic cell may be formed. Under those conditions, one of the metals presenting a lower corrosion potential would become the anode and corrode preferentially by galvanic corrosion, while the other metal would act as the cathode of the electrochemical cell (D. Jones 1996). The behaviour of a typical galvanic cell is schematically represented in Fig. 6.1.

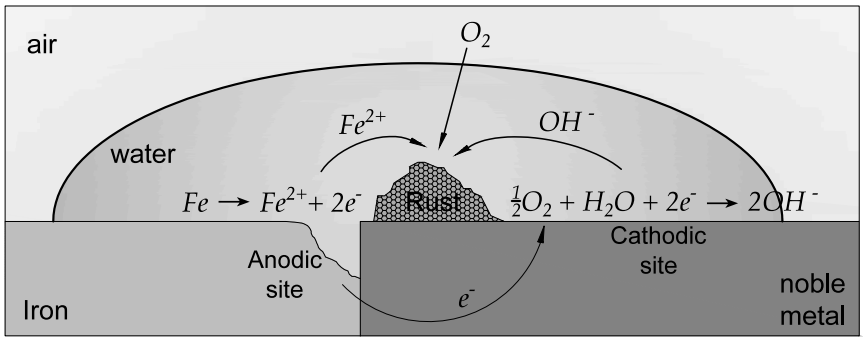

Figure 6.1: *Schematic representation of the behaviour of a typical galvanic cell*

Theoretically, galvanic corrosion may also arise in FRC structures between metallic fibres and conventional reinforcement where the concrete pore solution would act as the electrolyte, provided electrical connections are available. In the literature, studies can be found in which beneficial properties have been attributed to metallic fibres which were claimed to act as sacrificial anodes, thus protecting the reinforcing bars (Someh and Saeki 1997; Mihashi et al. 2011). Nevertheless, the opposite case, i.e. increased corrosion rate at the conventional reinforcement, is likewise feasible.

In order to study the risk of galvanic cells forming due to the different metals used for the fibres and reinforcing bars and to determine whether the cell formed would be beneficial or detrimental with regard to corrosion of the rebar, another type of experiment was designed and carried out in parallel to the long-term corrosion tests. The test programme is presented in Table 6.1.

6.1 Description

In reinforced concrete structures, concentration cells often occur, i.e. corrosion macro-cells are formed with separate anode and cathode sites due to variation of such factors as oxygen availability in the electrolyte (Bertolini et al. 2004). In FRC structures, some fibres will be located at the concrete cover between the reinforcement bars and the concrete surface and will therefore be more exposed to external agents. In chloride environments, given the increased corrosion resistance of steel fibres compared to conventional reinforcement,

Table 6.1: Experimental Programme

Galvanic corrosion experiments

Series	Concrete and fibre type		Fibre content % vol.	Number of specimens
Reference	Plain Concrete		-	3
Type A	SFRC	Low Carbon	0.5	3
			1.0	3
		Zinc Coated	0.5	3
			1.0	3
Type B		Low Carbon	0.5	3
			1.0	3
		Zinc Coated	0.5	-
			1.0	3

corrosion could start earlier at the reinforcement. Since the oxygen concentration would be higher near the concrete surface, the fibres could become localized cathodes with the rebar acting as the anode, provided there is electrical connection between the fibres and the rebar. On the other hand, fibres lying close to the surface might start corroding earlier if the chloride concentration is sufficiently high and, thereby, they could act as sacrificial anodes protecting the rebar.

For galvanic cells, two of the main factors controlling the corrosion rate are: (i) the differences in corrosion potential between the dissimilar metals and (ii) the ratio of the surface areas exposed to the electrolyte (D. Jones 1996). The first factor depends on both the type of metal and the electrolyte solution. Since the concrete pore solution is not expected to significantly vary from one specimen to another, the influence of the corrosion potential may be studied modifying the type of fibres. In the case of the second factor, the higher the fibre content, the higher the probability of creating electrical connections and of increasing the exposed surface ratio between the fibres and the rebar.

6.1.1 Test configuration

In order to consider the concentration or macro-cell effects in the test, three different series were cast: Reference, Type A and Type B, as seen in Fig. 6.2. The reference series were cast with plain concrete in order to use them as control specimens. Type A series were cast using SFRC, with the exception of the cover that was cast using plain concrete. Thus, different concentrations of oxygen or chloride at the fibres and rebar were avoided. Finally, the Type B series were fully cast using SFRC to include the effects of having different chloride and oxygen concentrations at the location of superficial fibres.

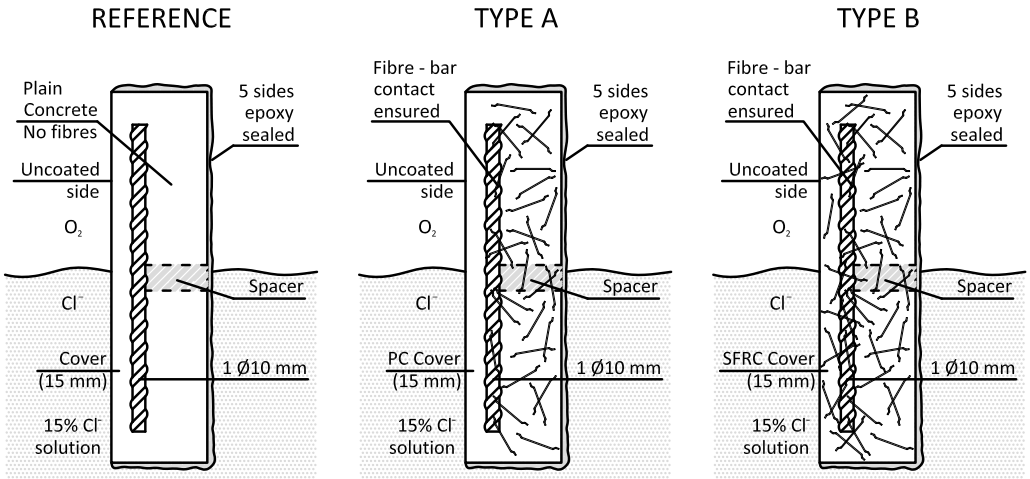

Figure 6.2: *Configuration of different series in the galvanic corrosion experiments*

6.1.2 Specimen design and materials

The specimens used in these experiments were 295 mm tall, 97 mm wide and 60 mm deep rectangular prisms, as presented in Fig. 6.3. Each specimen was cast with a single Ø10 mm embedded rebar used as received. A reduced clear concrete cover of only 15 mm was adopted to accelerate the initiation period.

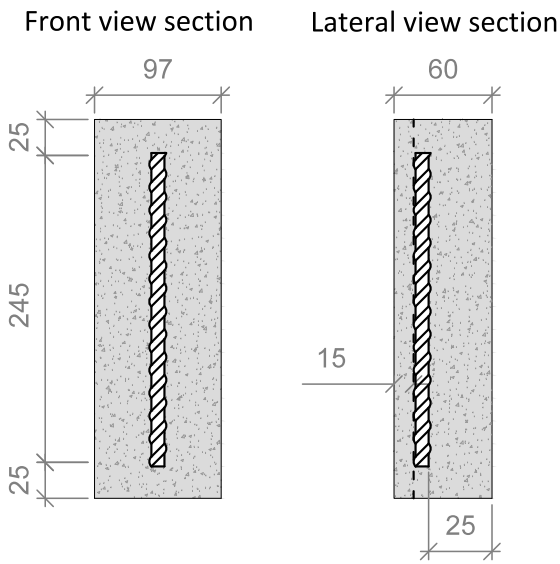

Figure 6.3: *Geometry of galvanic corrosion test specimens, measurements in mm*

Although the concrete mix proportions and w/c ratio used were the same as in the long-term corrosion experiments (see Table 4.5), two different types of metallic fibre were employed: end-hooked low-carbon steel fibres, the same as those used for the long-term experiments, and a zinc-coated corrosion resistant variant of the same shape and length. Two different fibre contents were investigated, 0.5% and 1.0% by volume of concrete.

6.1.3 Specimen preparation

All reinforcing bar segments were measured and weighed before casting. The specimens were then cast in a metallic mould in groups of three using a single plastic spacer placed at the centre of each rebar segment as shown in Fig. 6.4. The casting process was performed trying to ensure the electrical contact between the rebar and some fibres. The specimens in the Type A series were produced filling the moulds with SFRC until the rebars were completely embedded after which a 15 mm layer of plain concrete was cast wet on wet. After casting, the specimens were cured for 28 days, demolded and cut into three equal individual specimens using a rotating saw. Prior to the exposure to chlorides, five of the specimen faces were coated with epoxy-resin to prevent the ingress of moisture, oxygen and chlorides ions.

Figure 6.4: *Production process of specimens for the galvanic corrosion experiments*

6.1.4 Exposure conditions

Once the epoxy-coating had hardened, the specimens were introduced into a plastic box where they were partially immersed in 15% chloride solution up to approximately one half of their total height. The boxes were then covered with a plastic sheet to prevent evaporation of the solution and to keep a high relative humidity inside the box. The specimens in the galvanic corrosion experiments were continuously exposed to the chloride solution, as opposed to the specimens in the long-term corrosion tests. However, they were stored in the same room and were thus subjected to the same temperature variation.

6.1.5 Evaluation

At the end of the exposure period, the weight loss of the reinforcing bars will be measured by means of gravimetric analysis for all the specimens and the results will be compared to try to identify signs of a beneficial or pernicious effect of the fibres. Additionally, the extent of corrosion in terms of pit depth and corroded surface will be assessed and related to the state of the fibres located near the rebar.

7 Results

In this chapter, the most relevant results from the experimental programme carried out within this project are presented. Thereafter, the most important observations are highlighted and discussed.

7.1 Material tests

7.1.1 Compressive strength

In Fig. 7.1, the results from the compressive strength tests are presented for all concrete mixes used in this investigation, indicating the mean and standard deviation values for three specimens.

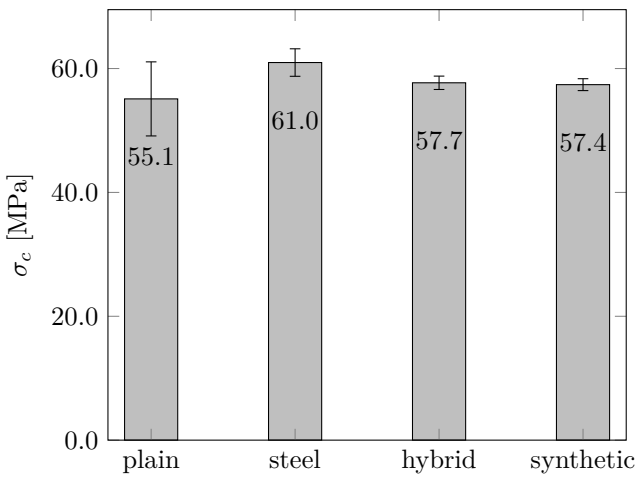

Figure 7.1: *Results of compressive strength for the different concrete mixes (mean values and standard deviation of three specimens)*

As observed in Fig. 7.1, the compressive strength of the concrete was not significantly influenced by the addition of fibre reinforcement, regardless of the fibre type.

7.1.2 Flexural tensile strength

Fig. 7.2 shows the flexural stress versus crack mouth opening displacement (CMOD) for all concrete mixes used in this investigation. The plotted curves represent the mean value over six specimens, except for plain concrete where only three beams were tested. The averaged coefficients of variance are presented in the legend.

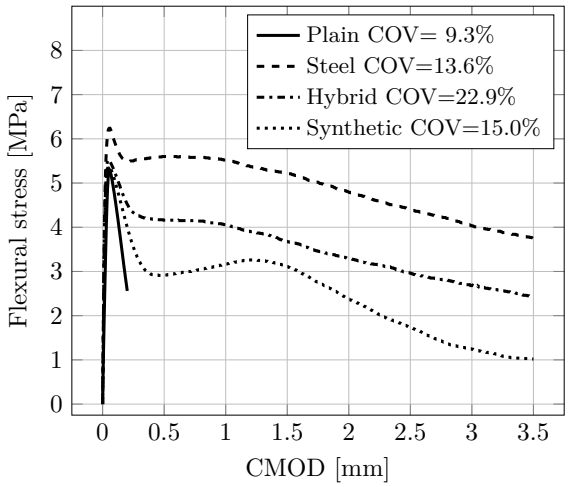

Figure 7.2: *Results of flexural tensile stress tests presented as flexural stress vs CMOD curves (mean values and standard deviation of six specimens, three for plain series)*

The results from the bending tests in terms of flexural strength resembled those obtained from compressive strength tests, i.e., a minor variation was observed throughout the different mixes. Conversely, the post-cracking behaviour was significantly affected by the addition of fibres, in that fibre reinforced concrete mixes displayed an improved toughness and residual flexural strength. Among the fibres used in these experiments, steel fibres showed the best performance results. However, it was observed that despite having used a 50% higher fibre dosage, the *Synthetic* series showed a significantly lower improvement of flexural behaviour. This finding suggested that much larger contents of PVA macro-fibres need to be used to achieve a similar response as that of SFRC, cf. (Kim and J.-Y. Lee 2011).

After performing the three-point bending tests, the notched beams were split into two halves separated by the crack formed during the test. Then, using digital images, the number of fibres on the crack surface was counted. Fig. 7.3 shows an example of the result for one of the halves of a beam specimen, in which the approximate position of the fibres on the crack surface can be observed. These results allowed an estimate of the average number of fibres crossing a section and thereby the fibre efficiency, as well as a calculation of the fibre distribution throughout the section height, which might later be correlated with the post-cracking behaviour of the specimens, see (Švec et al. 2014; P. A. Jones et al. 2007; Laranjeira de Oliveira 2010; da Cunha 2010).

7.1.3 Electrical resistivity

The results of the electrical resistivity tests are presented in Fig. 7.4 for all concrete mixes used in this investigation, indicating the mean and standard deviation values for three specimens.

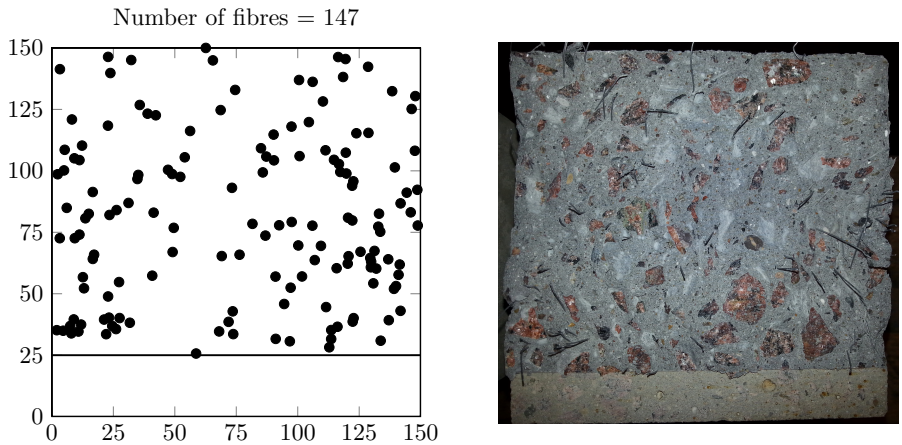

Figure 7.3: *Example of fibre distribution obtained through fibre counting on digital image*

According to the results shown in Fig. 7.4, steel fibres reduced the electrical resistivity of concrete, a reduction that was larger for higher contents. These results are in agreement with those reported by Solgaard et al. (Solgaard et al. 2013). Contrary to what the author had anticipated, the synthetic fibres used in this investigation, i.e. PVA fibres, also decreased electrical resistivity. Although the mechanisms causing this phenomenon have not yet been investigated, similar results have been reported in the literature (Kim, Boyd, et al. 2010).

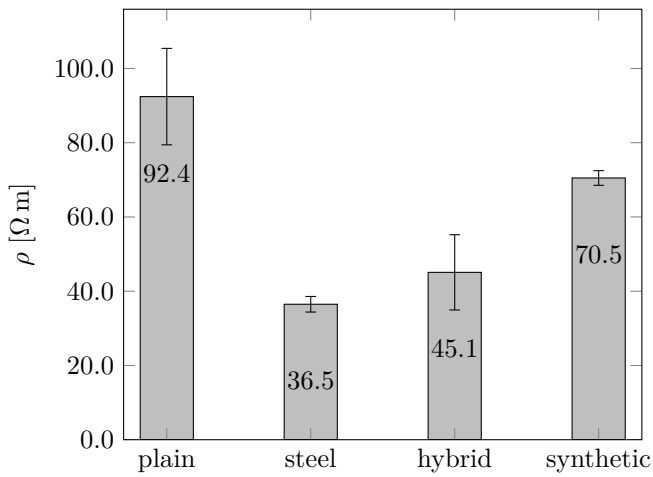

Figure 7.4: *Results of electrical resistivity for the different concrete mixes for saturated specimens (mean values and standard deviation of three specimens)*

7.1.4 Chloride migration coefficient

The chloride migration coefficient for all concrete mixes used in this investigation and obtained through the non-steady state migration tests are presented in Fig. 7.5, indicating the mean and standard deviation values for three specimens.

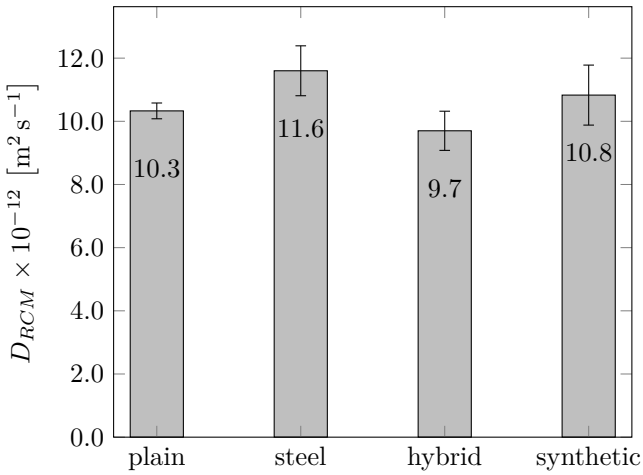

Figure 7.5: *Results of Rapid Chloride Migration Coefficient for the different concrete mixes (mean values and standard deviation of three specimens)*

Unlike electrical resistivity, the chloride migration coefficient did not seem to be significantly affected by the presence of fibres. This is in agreement with a number of observations by other researchers as discussed in Paper I.

7.1.5 Chloride diffusion coefficient

The chloride profiles for the different mixes obtained according to (EN 14629 2007) after seven months of exposure to a 10% chloride solution are shown in Fig. 7.6. The individual markers denote experimental observations whereas the continuous lines indicate the calculated profiles fitted by means of non-linear regression analysis to the Error Function (ERF) according to NT Build 443.

The most significant difference observed from these results was the variation of the surface chloride content between the *Plain* and *Steel* series and the *Hybrid* and *Synthetic* series. The former revealed larger chloride contents near the concrete surface leading to steeper gradients, whereas the latter presented a smoother chloride variation towards the inner zones of the specimen.

The solid lines in Fig. 7.6 represent the curves fitted to the experimental data according to the criteria specified in NT Build 443, i.e. the regression was performed starting

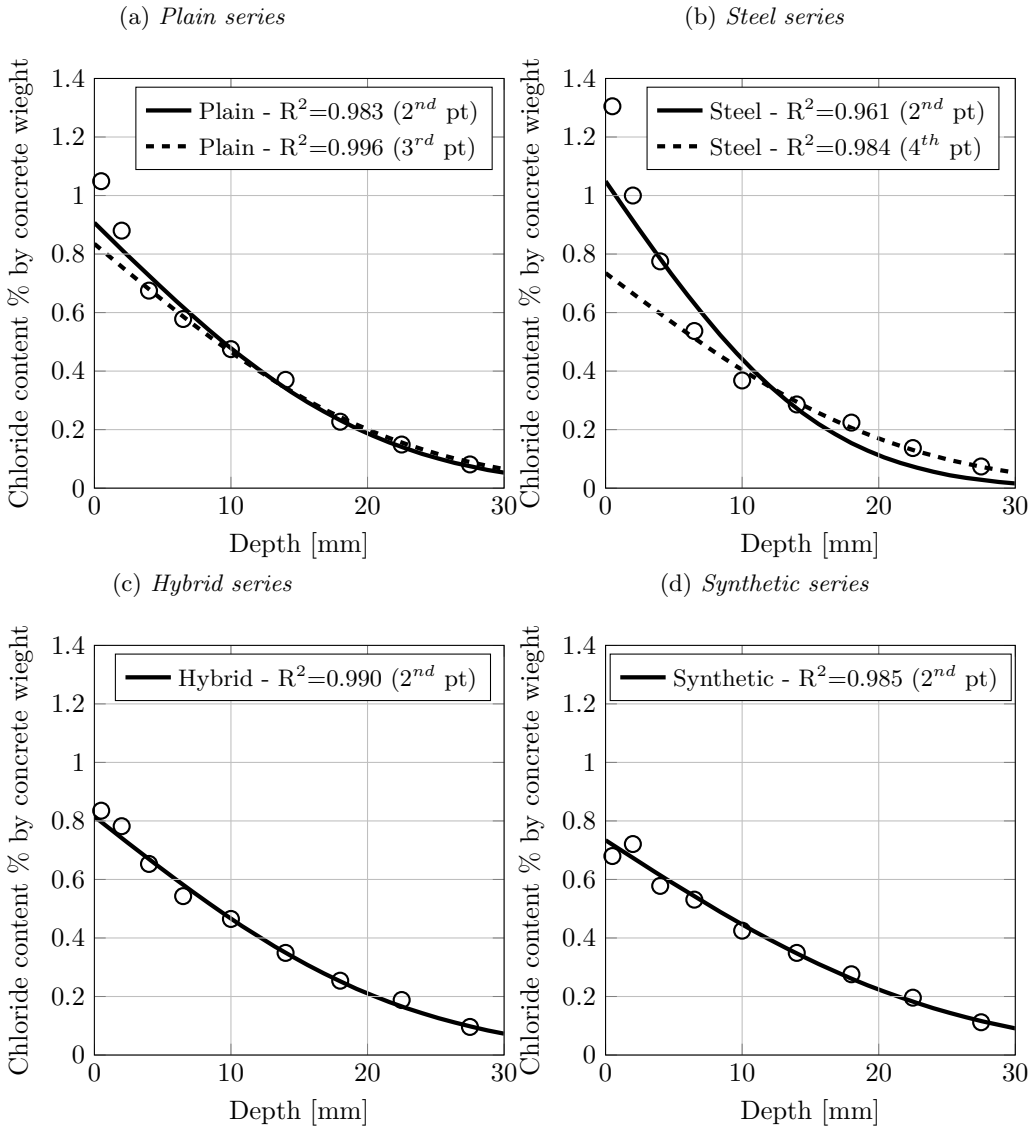

Figure 7.6: *Chloride content profile: experimental data points and fitted curves*

from the second most external point measured. In the case of the *Plain* and *Steel* series, this criterion led to a significantly higher surface chloride content and a relatively lower correlation coefficient.

In Fig. 7.7, the diffusion coefficients obtained through the migration tests are compared to the diffusion coefficients calculated from the regression analyses. As reported in

(Tang, Nilsson, et al. 2012), although the diffusion coefficients obtained from migration and immersion tests are comparable in most cases, slightly higher values are usually achieved from migration tests. Moreover, since the age of the specimens at the moment of starting the tests (45 and 211 days, respectively) and the duration of the tests (24 hours and 210 days, respectively) significantly differed, an ageing effect due to the hydration of concrete was also expected.

The first regression performed according to NT Build 443 yielded very low diffusion coefficients for the *Plain* and in particular for the *Steel* series compared to the other two series. Since the same concrete composition had been used for all specimens, there was no apparent reason for large variations of the surface chloride content. Therefore, the high chloride content found at the concrete surface of the *Plain* and *Steel* series might be attributed to the presence of voids or local defects in the concrete matrix near the surface. Thus, since the chloride content was similar in the inner zones for all mixes, the coefficients obtained seemed unrealistic.

A second regression analysis was performed starting at the third and fourth most external points measured for the *Plain* and *Steel* series, respectively. The resulting fitted curves are presented in Fig. 7.6 as dashed lines. The newly calculated surface chloride contents were in better agreement with the other mixes and the correlation coefficients increased as well. Similarly, the diffusion coefficients obtained through the second regression slightly increased, presenting smaller variations between the different mixes.

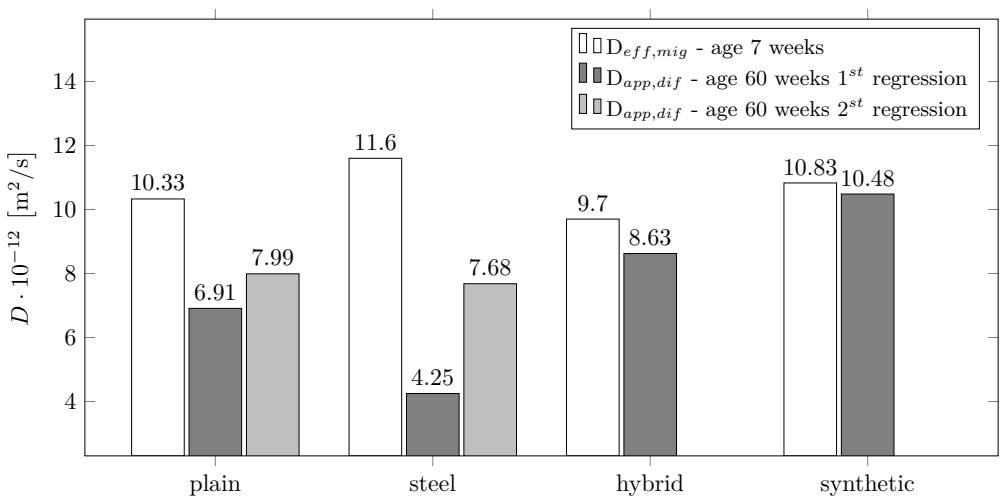

Figure 7.7: *Comparison between the effective diffusion coefficient obtained through migration tests and the apparent diffusion coefficient obtained through bulk diffusion tests*

7.2 Long-term corrosion experiments

7.2.1 Half-cell potential monitoring

In Fig. 7.8, a sample of the time variation of corrosion potential measured with the embedded reference electrode is presented versus a Copper Sulphate Electrode (CSE) for the different loading conditions. The values presented correspond to the central rebar of the specimens with a target crack width of 0.1 mm for all cracked series. Grey-shaded areas indicate periods of immersion in the chloride solution. The complete set of monitored half-cell potentials can be found in Appendix A.

It is interesting to note that the continuous monitoring of the half-cell potential accurately allowed the capture of the sudden drops of corrosion potential that are usually associated with the onset of active corrosion. Furthermore, a variation of the half-cell potential can be observed throughout the wetting and drying periods, possibly indicating changes in the resistivity of concrete and/or oxygen availability due to the moisture content variation in the vicinity of the reference electrode.

7.2.2 Corrosion initiation times

Half-cell potential measurements were used to determine the corrosion initiation times. In this investigation, the onset of corrosion was defined based on the suggestion by RILEM TC-235 CTC *"Corrosion Initiating Chloride Threshold Concentrations in Concrete"*, i.e., a sudden drop of half-cell potential by more than 150 mV per 24h and no re-passivation ocurring in the following seven days. A more detailed discussion of the half-cell potential interpretation can be found in Paper II.

Fig. 7.9 shows the corrosion initiation times for the different loading conditions. Each data point represents the average value for the two bars monitored in a beam specimen. The maximum crack width in the plots refers to the maximum crack width measured during the pre-loading procedure for the *Unloaded* and *Cyclic* series, whereas it refers to the maximum crack width measured in the re-loading procedure for the *Loaded* series.

It is noteworthy that the *Uncracked* series were excluded from Fig. 7.9 due to the fact that only a few reinforcing bars presented clear signs of active corrosion at the time of drafting this thesis. This fact confirms the major impact of cracks on the initiation of corrosion, since all cracked specimens had started to corrode after a period of 120 days while most bars in uncracked specimens seemed to remain passive after almost a year of exposure to the chloride solution.

(a) *Half-cell potential measurements for Uncracked series*

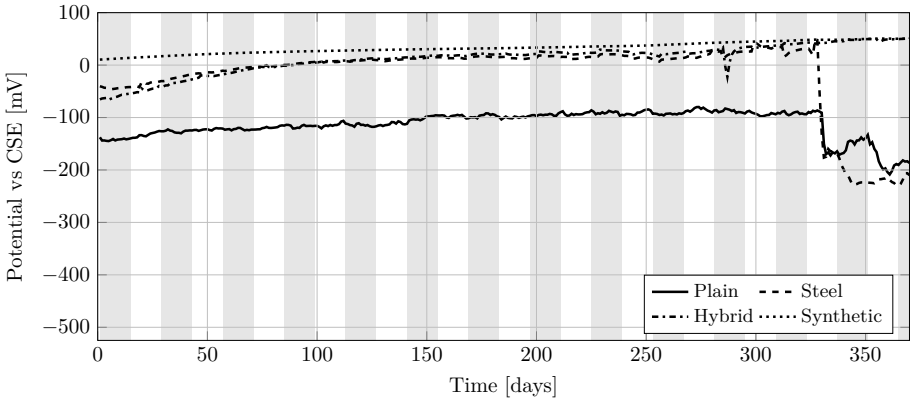

(b) *Half-cell potential measurements for Unloaded series*

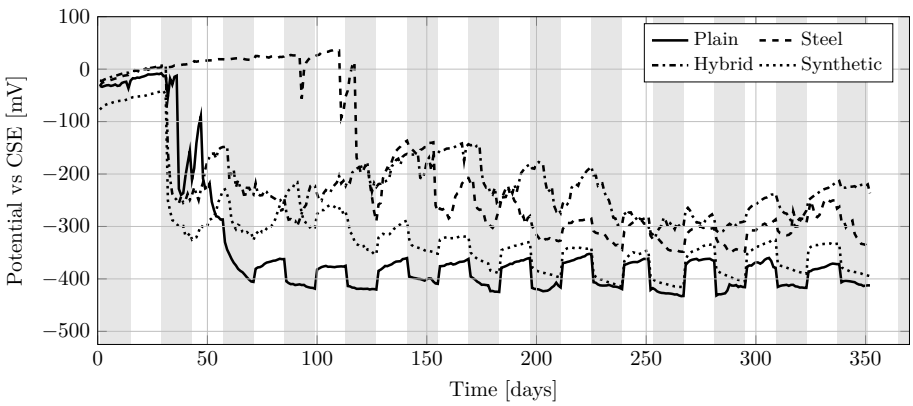

(c) *Half-cell potential measurements for Cyclic series*

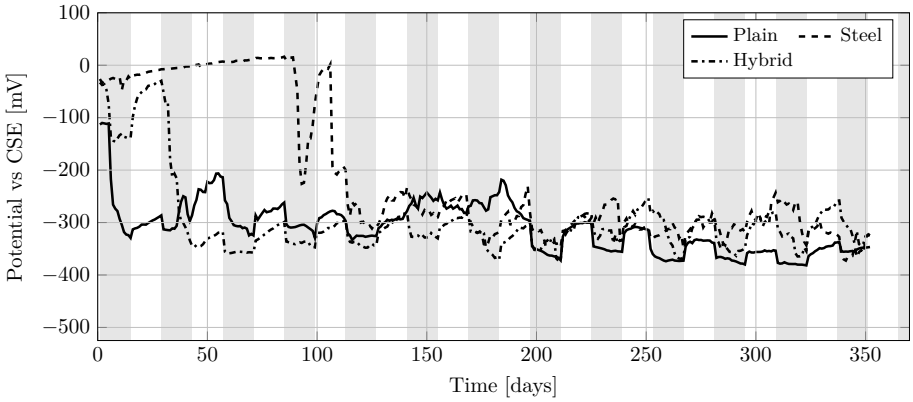

(d) *Half-cell potential measurements for Loaded series*

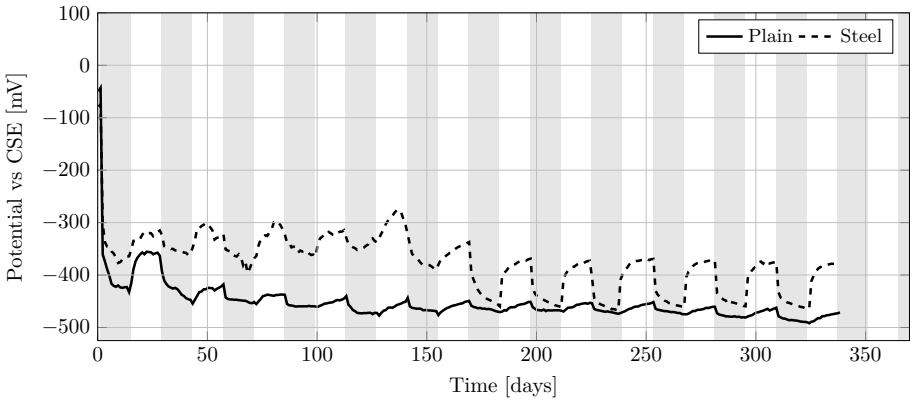

Figure 7.8: *Results of half-cell potential measurements from Unloaded, Cyclic and Loaded series. Gray-shaded areas indicate periods of immersion in the chloride solution.*

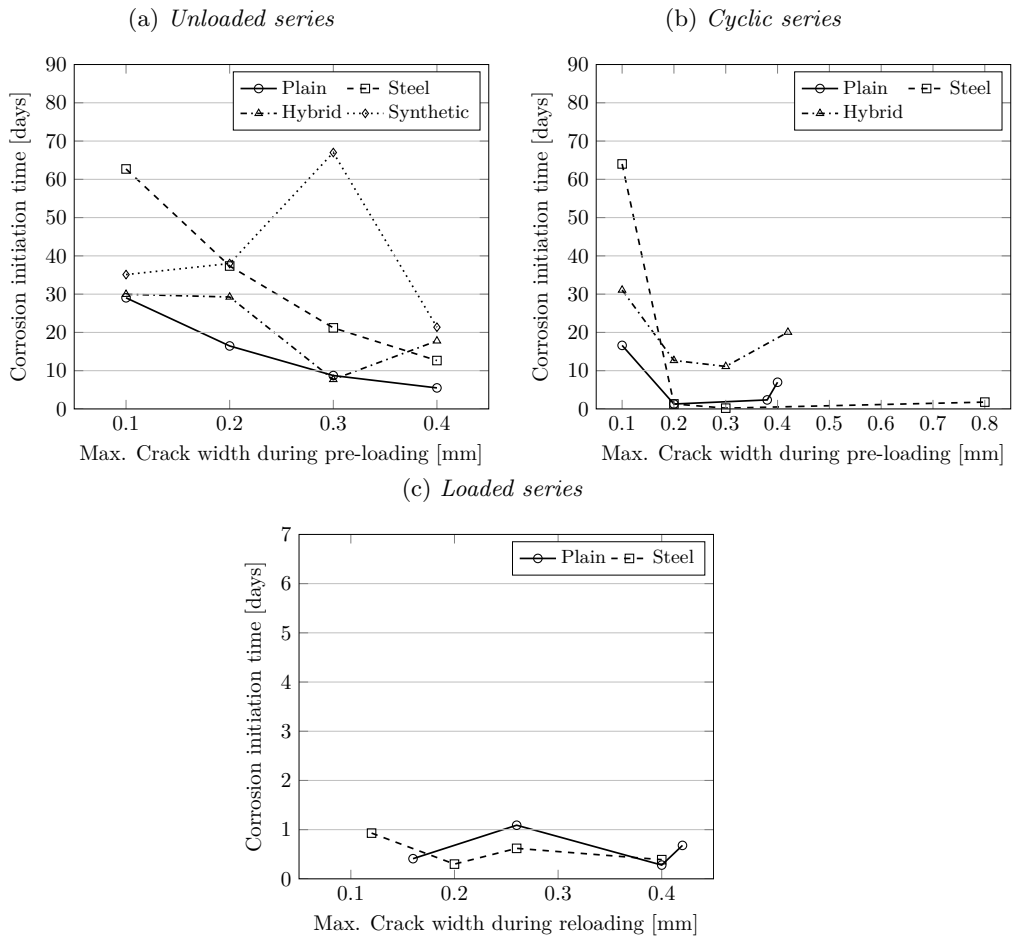

Figure 7.9: *Corrosion initiation times: influence of crack width. Note the different scales used in the ordinate axis in the* Loaded *series*

In the *Loaded* series, all the specimens with open cracks ranging from 0.1 to 0.4 mm started to corrode within the 48 hours that followed the first immersion in chloride solution. For the specimens in the *Unloaded* and *Cyclic* series, with closed cracks ranging from 0.02 to 0.06 mm, it took several days or even weeks for signs of corrosion to show. This significant difference in the initiation times suggested the existence of a crack width threshold, smaller than 0.1 mm for this investigation, above which the initiation period would be negligible. However, this threshold is most likely dependent on the cover depth and w/c ratio, among other parameters, and thus must not be extrapolated to other cases.

Despite the scatter found and the limited amount of specimens, a general trend could be observed for the *Unloaded* and *Cyclic* series, where specimens that had been subjected to larger crack widths during the pre-loading procedure yielded earlier corrosion initiation times. However, that trend could not be observed when plotting the corrosion initiation times vs the remaining crack width after unloading, which ranged between 0.02 and 0.06 mm, as shown in Fig. 7.10. This observation suggests that the actual surface crack width might not be the main parameter influencing the duration of the initiation period. The absolute maximum crack width reached during the entire load history of the structure, or similarly the maximum stress reached at the reinforcement, could be better indicators of a reduction in the corrosion initiation period. Alternatively, the interfacial damage between the concrete and the steel bars caused by mechanical loading might also better explain the variation in initiation times, which was supported by the fact that specimens subjected to five cycles of loading and unloading exhibited earlier corrosion compared to specimens that had been loaded only once, provided a certain load was exceeded.

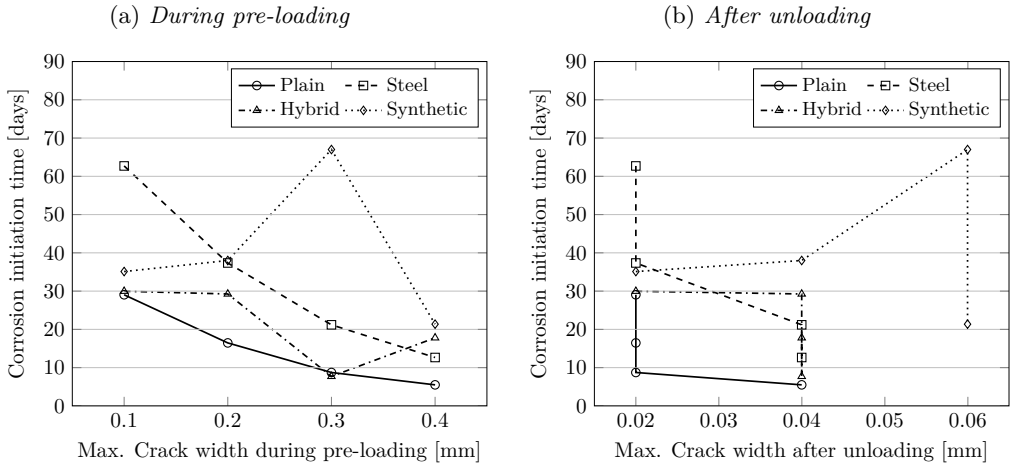

Figure 7.10: *Relation between the corrosion initiation times and the maximum crack width,* (a) *during pre-loading and* (b) *after unloading, for the* Unloaded *series. Note the different scale in the abicissa axis.*

On the other hand, the effect of the fibre type was less apparent. Steel fibres seemed to have a beneficial effect on the *Unloaded* series whereas this effect was only seen in the least loaded specimen in the *Cyclic* series and no effect could be observed in the *Loaded* series. Despite the lower elastic modulus of the PVA macro-fibres, the specimens in the *Synthetic* series, showed better performance for higher load levels. The reason for this is unclear. Although PVA fibres form a chemical bond with the cementitious matrix which might lead to a better crack closing effect after removing the load, such was not the case in this investigation (see Fig. 7.10b).

Considering that the general failure mode of uncorroded steel fibres is pull-out, as opposed to PVA fibres which tend to break, it might be argued that the damage caused by the slip of fibres, which is greater for higher load levels and cyclic loading, might have had a negative impact on the corrosion initiation period. However, it might also have been caused by the presence of local defects at the rebar and the limited number of specimens. The combination of steel macro-fibres and PVA micro-fibres used in the *Hybrid* series seemed less sensitive to cyclic loading, which suggested that if debonding is a decisive factor for corrosion initiation, adding PVA micro-fibres may arrest the bond-stress crack development better than steel macro-fibres alone, thereby delaying the onset of corrosion.

7.2.3 Corrosion rate

In Paper I, a number of investigations reporting the effect of steel fibres on the corrosion rate of conventionally reinforced concrete specimens are presented and discussed. The main observation from the studies reviewed was that steel fibres, *per se*, did not seem to influence the rate at which conventional reinforcement corroded. However, part of the investigations reported a beneficial effect of the fibres compared to plain concrete when corrosion-induced cracking occurred or when crack control was, in general, a critical issue.

A sample of the corrosion rate monitored with the help of the RapiCor device is presented in Fig. 7.11. The plotted data corresponds to the central reinforcing bar of the beams in the *Unloaded* series that were loaded to a maximum crack width of 0.2 mm. The evolution of the corrosion rate is presented for two different sections, in Fig. 7.11a for the mid-span section, where larger cracks developed during the loading procedure, and in Fig. 7.11b for a section near the support which remained above the water level and where no cracks developed.

It can be observed that in general, the corrosion rate monitored is subjected to a large variation during the period measured, independently of the addition of fibres. In Fig. 7.11, although the corrosion rate seems to increase more rapidly in the mid-span section, the data available is not sufficient to identify general patterns. Thus, further analysis is needed to draw conclusions regarding the influence of fibre reinforcement on the corrosion rate of conventional rebars.

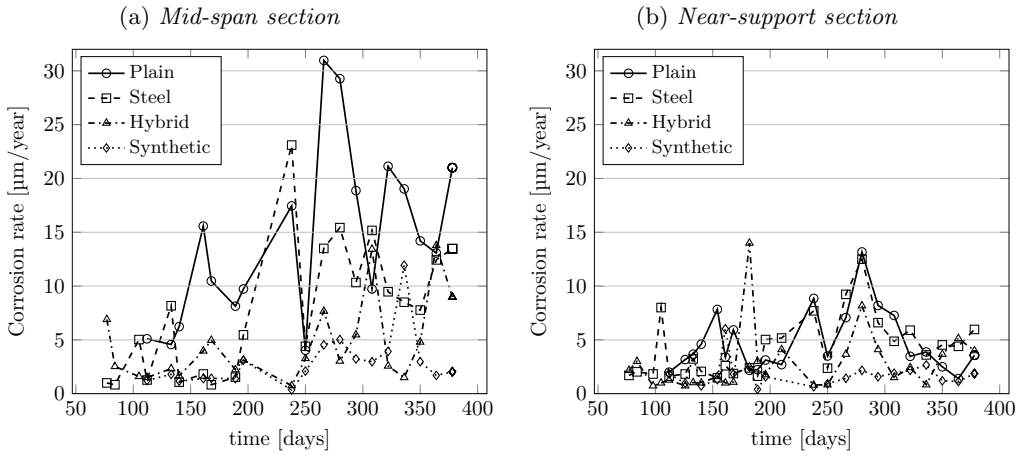

Figure 7.11: *Evolution of the corrosion rate in time for the central rebar at* (a) *the mid-span section and* (b) *a section near the support, for beams in the* Unloaded *series subjected to 0.2 mm maximum crack width during pre-loading.*

7.2.4 Corrosion of steel fibres

Steel fibres have been regarded in the literature as possessing an increased resistance to chloride-induced corrosion compared to conventional reinforcement. Steel fibres completely embedded in chloride contaminated concrete have been found to remain free of corrosion despite very high chloride contents. Nevertheless, low carbon steel fibres lying at the surface or bridging cracks may be readily corroded. It has been reported that in uncracked concrete, only the fibres located in the first millimetres of the concrete cover would corrode, possibly leading to conspicuous rust stains (Serna and Arango 2008). However, it has been found that the depth of the cover where fibres are affected can be significantly reduced by increasing the quality of the concrete (Balouch et al. 2010).

From the visual inspection of SFRC beams used in this investigation, despite the high chloride content in the solution, only isolated rust stains could be spotted on the surface of the beams after a year of cyclic exposure. This is shown in Fig. 7.12, where the surface state of beams belonging to the different series, after a year of chloride exposure, is presented. The reduced amount of rust observed on the surface might be attributed, to some extent, to the wetting-drying exposure conditions which might have washed out the corrosion products from the surface of the beams.

A difference was noticed, however, between the top face of the beams (not in contact with the formwork during the casting procedure), where it was impossible to prevent some fibres from sticking out, and all the other faces. In the former, the fibres started to corrode almost immediately after being in contact with chlorides while in the remaining surfaces it took longer for the rust stains to appear.

(a) Plain *series*

(b) Steel *series*

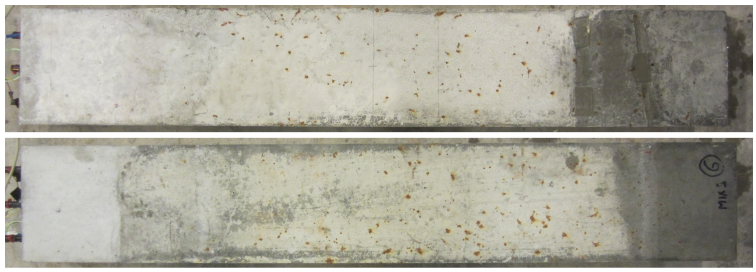

(c) Hybrid *series*

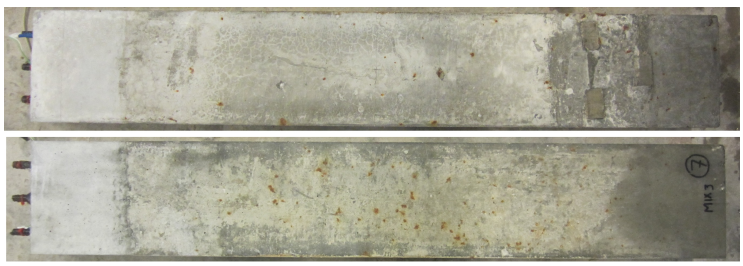

(d) Synthetic *series*

Figure 7.12: *State of the beam surfaces for the different series after a year of cyclic exposure to chloride solution.*

7.3 Modelling of chloride ingress

As already mentioned, the corrosion initiation period comprises the time needed for depassivating agents to penetrate the concrete cover and accumulate at the reinforcement level until a critical quantity, necessary to break down the passive layer, has been reached. Thus, the modelling of chloride ingress into concrete constitutes one of the key aspects in the service life analysis of reinforced concrete structures.

The ingress of chloride into concrete usually involves more than one transport mechanism. However, the influence of the different transport mechanisms is commonly treated together, considering the ingress of chlorides as the result of a diffusion process solely. Using this simplification, Collepardi (Collepardi et al. 1970) first introduced in the 1970s the simple ERFC model based on the complementary error function, denoted *erfc*, to describe the ingress of chloride into concrete according to Fick's Second Law of Diffusion.

Since then, a number of emperical models based on the same complementary error function have been developed to include the time-dependency of the parameters involved. Other more sophisticated models accounting for physical and chemical processes involved in the transport of chloride in concrete, so-called physical models, are also available. Although the majority of widely used models are in practice based on the error function, other models exist which are based on different analytical solutions to the Fick's Laws of Diffusion, cf. (Nilsson 2001).

In this study, two different models were used to predict the chloride ingress into concrete and to compare the results with the experimental data obtained through the bulk chloride diffusion tests performed. The models selected were the DuraCrete model and the ClinConc model (Tang 2008). The DuraCrete model for chloride ingress is an empirical model that includes the time-dependency of the diffusion coefficient and that considers a constant chloride surface content. The ClinConc model is regarded as a physical model since it uses free chlorides as the driving potential for the diffusion process and then calculates the distribution of total chlorides considering the binding capacity of concrete based on the concept of the binding isotherm. In the ClinConc model, both the diffusivity and binding capacity are regarded as time-dependent parameters.

In Fig. 7.13, the chloride ingress profiles predicted according to the DuraCrete and the ClinConc models, after 210 days of exposure, are compared to the experimental data measured from the *Plain* series. Note that the experimental data was determined as chloride content by weight of concrete, but it is here expressed as chloride content by mass of cement. This value was calculated based on the mix design since the cement content of the samples has not been determined yet. The input parameters for the DuraCrete and ClinConc models are presented in Table 7.1 and Table 7.2, respectively.

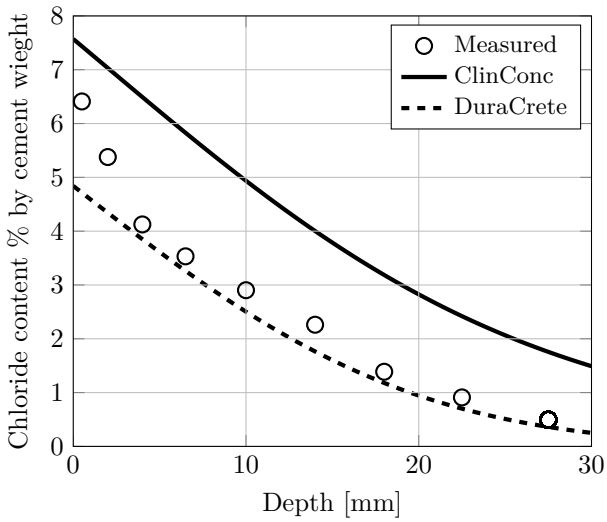

Figure 7.13: *Chloride ingress prediction according to ClinConc and DuraCrete models compared to experimental data*

Table 7.1: Input parameters for the DuraCrete model

Water cement ratio, [−]	w/c	0.47
Surface chloride content regression parameter. [% binder mass]	$A_{c_s,cl}$	10.3
Curing factor, [−]	$k_{c,cl}$	0.79
Environment factor, [−]	$k_{e,cl}$	1.32
Age factor, [−]	n_{cl}	0.30
Diffusion coefficient, [m^2/s]	D_0	$10{\cdot}10^{-12}$
Time meas. D_0, [days]	t_0	45

Fig. 7.13 shows that the DuraCrete model yielded a prediction which is in good agreement with the experimental data. As previously mentioned, the DuraCrete model considers a constant surface chloride content which is dependent on the quality of concrete and the environmental conditions through the w/c and the regression parameter $A_{c_s,cl}$, respectively. The input data for the model calibration was obtained from concrete structures made of ordinary portland cement, as well as sulphate resistant portland cement (SRPC), cf. (Brite EuRam 1999; Sandberg 1998), similar to that used in the experiments. Thus, the binding capacity of the concrete could probably be well described by the model. However, the calibration of the model was also performed for use in natural marine environments, which present a much lower salinity than that of the solution used in the experiments. On the other hand, the temperature of the salt solution exposed to the laboratory conditions was, most likely, significantly higher than the average temperature of the sea. Therefore, the expectedly high surface chloride content caused by the high concentration of salt in

Table 7.2: Input parameters for the ClinConc model

w/c [−]	Cement content kg/m^3	Air content %	Porosity %	$[OH]_{6m}$ mol/l	c_s g/l	c_i g/l	Temp. °C
0.47	360	3.0	11.3	0.53	119	0.021	21

Diffusivity, D_{mig} $\cdot 10^{-12}$ m^2/s	Time meas. D_{mig} days	Time dependency D [−]	Age exposure days
10	45	$\beta_t = 0.152 \cdot (w/c)^{-0.6}$	211

Binding Isotherm Slope	Binding Non-linear exponent	Factor binding time dependency
f_b=3.6	β_b=0.38	$f_t = 0.36ln(t_{cl} + 0.5) + 1$

the exposure solution could have been offset by a lower binding capacity due to a fairly high and constant temperature in the laboratory, resulting in a good agreement between the experiments and the prediction. Nevertheless, if the surface chloride content may vary in time (Uji et al. 1990), the agreement for future predictions using might be reduced.

The resulting chloride ingress profile predicted by the ClinConc model significantly overestimated the chloride content throughout the entire cover depth. As in the previous case, the ClinConc model has been calibrated for chloride concentrations lower than one molar ($\sim$ 35 g/l) and, due to the lack of more specific input data, the parameters regarding the binding capacity of concrete used in the analysis were those recommended for OPC, not for SRPC. However, since the actual concentration in the solution and temperature were used for the ClinConc model prediction, the two effects were not evened out.

In a report from the Road Directorate of Denmark (Nilsson, Sandberg, et al. 1997), the ability of the ClinConc model to predict the chloride ingress of specimens tested according to the NT Build 443 was investigated. Similar results were obtained in which the ClinConc model overestimated the chloride content determined experimentally. Two phenomena were identified as possible causes of the disagreement between the model and the experiments: i) a different age-dependency of the "*true*" diffusion coefficient compared to the migration coefficient used as input for the model and ii) a concentration dependency of the chloride diffusion coefficient as described in (Nilsson, Poulsen, et al. 1996), where high chloride concentrations might lead to reduced diffusion coefficients.

Nonetheless, the available results indicate that for short-term exposure to a high chloride concentration, the ClinConc model is not capable of capturing the chloride ingress behaviour and the driving potential (i.e. the chloride concentration in the pore solution) is overestimated.

7.4 Concluding discussion

The experiments presented aimed at investigating whether the addition of fibre reinforcement, at low dosages, would influence some of the parameters regarded as decisive for the corrosion of steel bars in concrete and how the corrosion initiation and propagation periods would be affected by the presence of fibres.

Although it has been established that fibres would feature an interfacial transition zone similar to that formed around aggregates (S. F. Lee and Jacobsen 2011) and despite the significant amount of additional surface provided by the fibres, the transport properties in terms of chloride migration and bulk diffusion did not seem to be significantly influenced.

The resistivity of concrete, due to its great dependence on the moisture content and pore network characteristics (size, connectivity, etc.), has sometimes been used as an indicator of concrete diffusivity. In the *Synthetic* series, the reduction of electrical resistivity could be associated with a slightly higher diffusion coefficient, which could be attributed to the hydrophilic nature of the PVA fibres, i.e. the capacity to absorb moisture. However, no difference was observed regarding the chloride migration coefficient compared to plain concrete specimens. Given the time lag between the moment when the migration and diffusion tests were performed, the higher diffusion coefficient might be explained by the prolonged exposure to chlorides, which could have crystallized causing some degradation of the PVA fibres and, thus, increasing ion diffusivity. Nevertheless, if the same relation between resistivity and diffusion were to be applied on concrete containing steel fibres, based on the resistivity measurements, the diffusion coefficient would be expected to have been significantly raised. However, as observed, the *Steel* series displayed the lowest chloride diffusion coefficient. This fact suggests that in the resistivity tests, the steel fibres increased the conductivity but did not increase the flow of ionic species through the pore network of the concrete matrix but, instead, the current applied travelled by electron transfer within the conductive fibres.

Different opinions exist regarding the influence that the reduced resistivity measured in SFRC might have on the corrosion rate of steel bars if these two types of reinforcement were used together. Whereas some researchers affirm that only the electric current travelling as ionic flow through the concrete matrix would influence the corrosion rate, others claim that electronic transfer within the steel fibres would yield a negative impact.

The premise that fibre reinforcement could be an effective way to control crack width in concrete elements with conventional reinforcement was supported by the results obtained during the pre-cracking procedure. However, since all specimens were loaded to obtain an equal surface crack width, the impact of the improved crack control of FRC could not be directly observed on the corrosion initiation period for the long-term corrosion experiments. Nevertheless, despite having been subjected to larger loads, all fibre reinforced specimens, showed similar or better performance with respect to corrosion initiation than their plain concrete counterparts, regardless of the type of fibre or loading conditions applied.

8 Conclusions

This study was aimed at investigating whether fibres, due to their crack limiting effect, could improve the durability of reinforced concrete structures affected by chloride-induced corrosion. Through an initial review of the existing literature, presented in Paper I, the influence of fibre reinforcement on relevant factors governing the corrosion of steel bars in concrete was investigated. The literature review also enabled the identification of some key aspects that remain unclear or need further investigation regarding the corrosion of steel bars in FRC. Finally, in order to gain a better understanding of how fibres might influence the corrosion of steel bars and to shed some light on the questions that have not yet been investigated, an experimental programme was developed.

8.1 General conclusions

From the literature review, it was concluded that the addition of steel fibres into concrete, even at small dosages, could arrest the development of cracks in conventionally reinforced concrete, resulting in narrower cracks. This finding was experimentally verified in this investigation while performing the pre-cracking procedure of the beam specimens. Moreover, by controlling the development of splitting cracks around the reinforcing bars, steel fibres might reduce the bond degradation between the bars and the concrete matrix.

Given the direct relationship between crack width and permeation, where the flow through a crack depends on the cube of the crack width, and owing to the increased crack control provided by the fibres, FRC has reportedly exhibited enhanced water tightness compared to plain concrete, in cracked state.

All investigations reviewed agreed on the fact that adding steel fibres to the concrete would result in a lower measured electrical resistivity. The degree of saturation of concrete, however, seemed to have a higher impact on resistivity than adding steel fibres at low dosages. Chloride diffusion on the other hand, would not be significantly affected by the presence of fibres. These observations were later supported by the experimental results obtained through different tests carried out during the course of this project.

The monitoring of half-cell potential performed during the long-term corrosion experiments revealed that all cracked specimens started to corrode within the 120 days that followed the first immersion in the 16.5% NaCl solution. However, uncracked specimens remained free of corrosion after a twice as long period and even after a year of exposure, only part of the specimens showed signs of active corrosion. This time difference highlighted the fundamental role that cracks play in the corrosion process of reinforcement, which was found to be independent of the addition of fibres.

From the analysis of the corrosion initiation times, two distinct behaviours were observed regarding the influence of varying the crack width. On the one hand, steel bars started to corrode almost immediately when the surface cracks were kept open above a

certain critical width. This observation suggested the existence of a crack width threshold, found to be smaller than 0.1 mm for this investigation, above which the initiation period could be, in practice, disregarded. On the other hand, significant differences were observed in the initiation periods of steel bars embedded in specimens with similar surface crack widths. This observation suggested that some other factors might be more decisive in prolonging the corrosion initiation period in reinforced concrete structures than surface crack width. Given the trend found, where corrosion started earlier for highly loaded specimens or specimens subjected to cyclic loading, one of these factors could be related to the interfacial damage caused between the bars and the concrete matrix during mechanical loading.

The addition of fibres to the concrete did not seem to have a significant effect on the corrosion initiation period, although a slight improvement could be observed in some cases. Overall, fibre reinforced specimens evidenced a similar or better performance than plain concrete specimens with regard to corrosion initiation.

From the experimental results included in the literature review, no evidence was found that steel fibre reinforcement would significantly increase the corrosion rate of conventional steel bars embedded in concrete under chloride attack. In most cases, the corrosion rate seemed to remain unaffected by the presence of steel fibres or else a reduction was observed which might be attributed to an improved control of corrosion-induced cracks.

There are, however, some aspects in which steel fibres may have a negative impact. Firstly, the rust stains caused by the corroding fibres lying at the concrete surface may give a bad aesthetical impression, posing an impediment for SFRC to be used in concrete elements with exposed surfaces. Additionally, although corrosion-induced cracking and spalling of the concrete are processes that promote accelerated degradation of the structure, they are unequivocal signs of the underlying problem. However, in FRC the improved crack control provided by the fibres might arrest the development of wide cracks that could delay or even hide the signs revealing the real state of the structure. Furthermore, commonly used methods for corrosion assessment of reinforced concrete structures rely on polarization techniques. Measurements performed using these techniques have been reported to grossly overestimate the actual corrosion rate in SFRC, yielding misleading conclusions of the real condition of the reinforcement.

8.2 Suggestions for future research

As discussed in Paper I, the effectiveness of fibre reinforcement, even at low dosages, to reduce the crack width in conventionally reinforced concrete elements has been reported by several authors. However, this beneficial effect of fibres has been mostly based on observations of surface crack width. As previously mentioned, it has been hypothesized by other researchers that the condition of the reinforcement interface or the crack width at the reinforcement level might be more important indicators of the susceptibility of steel bars for early corrosion, which was supported by some of the results obtained in this project. Therefore, it would be interesting to investigate whether and how low contents

of fibre reinforcement added to normal strength concrete could significantly modify the crack profile in elements with conventional reinforcement.

One of the main questions that still remains unclear is whether the low electrical resistivity measured in SFRC compared to plain concrete would negatively affect the corrosion rate of conventional reinforcing bars. This particular topic has already been investigated but the conclusions of different authors are contradictory. While some researchers claim that the presence of steel fibres would result in higher corrosion rates, others argue that only the current transferred in the form of ionic flow would contribute to the corrosion rate. Therefore, there is a need for further experimental research in order to try to find evidence to discern the actual role of the conductivity of steel fibres on the corrosion rate of conventional rebar .

As it happens when two dissimilar metals are in contact, the combined use of steel fibres and reinforcing bars raises questions regarding the risk of galvanic corrosion. A few investigations mentioned the possible formation of a galvanic cell between the metallic fibres and the steel reinforcing bars where fibres could have acted as sacrificial anodes, thus reducing the rate of corrosion at the main reinforcement. However, this mechanism could in practice proceed in the opposite direction, i.e. steel fibres could increase the rate of corrosion of steel bars. Nevertheless, studies specifically aimed at investigating this effect have not been found in the literature and, therefore, the extent to which galvanic corrosion might be relevant and the conditions under which this type of corrosion might be promoted are still unclear.

One of the drawbacks of using FRC in conventionally reinforced concrete structures susceptible to corrosion could be the delay or absence of corrosion-induced cracks or spalling of the concrete cover which might hide the signs of an advanced state of corrosion of the reinforcement. However, to the author's knowledge, the requirements, on fibre reinforcement and cover depth, for fibres to prevent corrosion-induced spalling-cracks in normal strength concrete have not been specifically studied. This could be investigated experimentally or by using available numerical models which could simulate the inner tensile stresses produced by the accumulation of expansive corrosion products.

References

ACI Committee 318 (2011). *318-11: Building Code Requirements for Structural Concrete and Commentary*.

Andrade, C., Muñoz, A., and Torres-Acosta, A. (2010). "Relation between crack width and corrosion degree in corroding elements exposed to the natural atmosphere". In: *framcos.org*, pp. 853–858.

Arya, C. and Ofori-Darko, F. (1996). "Influence of crack frequency on reinforcement corrosion in concrete". In: *Cement and Concrete Research* 26.3, pp. 345–353. ISSN: 00088846. DOI: 10.1016/S0008-8846(96)85022-8.

Balouch, S., Forth, J., and Granju, J.-L. (2010). "Surface corrosion of steel fibre reinforced concrete". In: *Cement and Concrete Research* 40.3, pp. 410–414. ISSN: 00088846. DOI: 10.1016/j.cemconres.2009.10.001.

Bardal, E. (2004). *Corrosion and Protection*. Ed. by E. Bardal. Engineering Materials and Processes. London: Springer London. ISBN: 978-1-85233-758-2. DOI: 10.1007/b97510.

Beeby, A. W. (1978). "Cracking: what are crack width limits for?" In: *Concrete* 12.7, pp. 31–33.

Bentur, A. and Mindess, S. (2007). *Fibre reinforced cementitious composites*. 2nd. Abingdon, United Kingdom: Taylor & Francis, p. 601.

Bertolini, L., Elsener, B., Pedeferri, P., and Polder, R. (2004). *Corrosion of Steel in Concrete. Prevention, Diagnosis, Repair*. Weinheim, Germany: Wiley-VCH Verlag GmbH & Co. KGaA, p. 392. ISBN: 3527308008.

Blanco, A. (2013). "Characterization and modelling of SFRC elements". PhD thesis. Universitat Politècnica de Catalunya, p. 167.

Blunt, J. D. (2008). "The Effect of Fiber Reinforcement on the Corrosion Controlled Degradation of Reinforced Concrete Flexure Elements". PhD thesis. University of California, Berkeley, p. 201.

Brite EuRam (1999). *Quantification of the environmental parameters in the carbonation and chloride ingress models -Report BE95-1347/TG4/C*. Tech. rep., p. 94.

Broomfield, J. (2002). *Corrosion of steel in concrete: understanding, investigation and repair*. 2nd Ed. Abingdon, United Kingdom: Taylor & Francis, p. 277. ISBN: 0203414608.

Collepardi, M., Marcialis, A., and Turriziani, R. (1970). "The kinetics of chloride ions penetration in concrete (in Italian)". In: *Cemento* 67, pp. 157–164.

da Cunha, V. M. d. C. F. (2010). "Steel Fibre Reinforced Self-Compacting Concrete (from Micro-Mechanics to Composite Behaviour)". PhD thesis. University of Minho, p. 365. ISBN: 9789728692445.

Dauberschmidt, C. (2006). "Untersuchungen zu den Korrosionsmechanismen von Stahlfasern in chloridhaltigem Beton". PhD thesis. Technischen Hochschule Aachen, p. 163.

de la Fuente, A., Pujadas, P., Blanco, A., and Aguado, A. (2012). "Experiences in Barcelona with the use of fibres in segmental linings". In: *Tunnelling and Underground Space Technology* 27.1, pp. 60–71. ISSN: 08867798. DOI: 10.1016/j.tust.2011.07.001.

di Prisco, M., Plizzari, G., and Vandewalle, L. (2009). "Fibre reinforced concrete: new design perspectives". In: *Materials and Structures* 42.9, pp. 1261–1281. ISSN: 1359-5997. DOI: 10.1617/s11527-009-9529-4.

Edvardsen, C. (1999). "Water Permeability and Autogenous Healing of Cracks in Concrete". In: *ACI materials Journal* 96.4.

Elsener, B., Klinghoffer, O., Frolund, T., Rislund, E., Schiegg, Y., and Böhni, H. (1997). "Assessment of Reinforcement Corrosion by means of Galvanostatic Pulse Technique". In: *International Conference Repair of Concrete Structures*. Svolvær, Norway.

EN 12390-2 (2009). *EN 12390-2:2009 Tesing hardened concrete - Part 2: Making and curing specimens for strength tests.*

EN 12390-3 (2009). *EN 12390-3:2009 Testing hardener concrete. Part 3: Compressive strength of test spcimens.*

EN 14629 (2007). *EN 14629:2007 Products and systems for the protection and repair of concrete structures - Test methods - Determination of chloride content in hardened concrete.*

EN 14651 (2007). *EN 14651:2007 Test method for metallic fibered concrete - Measuring the flexural tensile strength (limit of proportionality (LOP), residual)*. Brussels, Belgium.

EN 1992-1-1 Eurocode 2 (2004). *EN 1992-1-1 Eurocode 2: Design of concrete structures - Part 1-1: General rules and rules for buildings*. Brussels, Belgium.

EN 206-1 (2000). *EN 206-1 Concrete - Part 1: Specification, performance, production and conformity*. Tech. rep., pp. 1–72.

Fantilli, A. P., Mihashi, H., and Vallini, P. (2007). "Crack profile in RC, R/FRCC and R/HPFRCC members in tension". In: *Materials and Structures* 40.10, pp. 1099–1114. ISSN: 1359-5997. DOI: 10.1617/s11527-006-9208-7.

fib Model Code for Concrete Structures (2010). Vol. 14. 3. Weinheim, Germany: Wiley-VCH Verlag GmbH & Co. KGaA. ISBN: 9783433604090. DOI: 10.1002/9783433604090.

Geiker, M. R. (2012). "On the importance of execution for obtaining the designed durability of reinforced concrete structures Dedicated to Professor Dr . Bernhard Elsener on the occasion of his 60th birthday". In: 12, pp. 1114–1118. DOI: 10.1002/maco.201206754.

Ghods, P. (2010). "Multi-Scale Investigation of the Formation and Breakdown of Passive Films on Carbon Steel Rebar in Concrete". PhD thesis. Carleton University, p. 322. ISBN: 9780494678855.

Hobbs, D. (2001). "Concrete deterioration: causes, diagnosis, and minimising risk". In: *International Materials Reviews* 46.3, pp. 117–144. ISSN: 0950-6608. DOI: 10.1179/095066001101528420.

Jaffer, S. and Hansson, C. (2008). "The influence of cracks on chloride-induced corrosion of steel in ordinary Portland cement and high performance concretes subjected to different loading conditions". In: *Corrosion Science* 50.12, pp. 3343–3355. ISSN: 0010938X. DOI: 10.1016/j.corsci.2008.09.018.

Janotka, I., Krajcí, L., Komlos, K., and Frtalová, D. (1989). "Chloride corrosion of steel fibre reinforcement in cement mortar". In: *The International Journal of Cement Composites and Lightweight Concrete* 11.4, pp. 221–228.

Jansson, A., Lofgren, I., Lundgren, K., and Gylltoft, K. (2012). "Bond of reinforcement in self-compacting steel-fibre-reinforced concrete". In: *Magazine of Concrete Research* 64.7, pp. 617–630. ISSN: 0024-9831. DOI: 10.1680/macr.11.00091.

Jones, D. (1996). *Principles and prevention of corrosion*. 2nd. Prentice Hall, p. 583. ISBN: 0133599930.

Jones, P. A., Austin, S. A., and Robins, P. J. (2007). "Predicting the flexural load–deflection response of steel fibre reinforced concrete from strain, crack-width, fibre pull-out and distribution data". In: *Materials and Structures* 41.3, pp. 449–463. ISSN: 1359-5997. DOI: 10.1617/s11527-007-9327-9.

Kim, B., Boyd, a. J., and Lee, J.-. Y. (2010). "Effect of transport properties of fiber types on steel reinforcement corrosion". In: *Journal of Composite Materials* 45.8, pp. 949–959. ISSN: 0021-9983. DOI: 10.1177/0021998310380286.

Kim, B. and Lee, J.-Y. (2011). "Relationships between mechanical and transport properties for fiber reinforced concrete". In: *Journal of Composite Materials* 46.13, pp. 1607–1615. ISSN: 0021-9983. DOI: 10.1177/0021998311421691.

Laranjeira de Oliveira, F. (2010). "Design-oriented constitutive model for steel fiber reinforced concrete". PhD thesis. Universitat Politècnica de Catalunya, p. 218.

Lee, S. F. and Jacobsen, S. (2011). "Study of interfacial microstructure, fracture energy, compressive energy and debonding load of steel fiber-reinforced mortar". In: *Materials and Structures* 44.8, pp. 1451–1465. ISSN: 1359-5997. DOI: 10.1617/s11527-011-9710-4.

Li, V. and Leung, C. (1992). "Steady-state and multiple cracking of short random fiber composites". In: *Journal of Engineering Mechanics* 118.11, pp. 2246–2264.

Löfgren, I. (2005). "Fibre-reinforced concrete for industrial construction - a fracture mechanics approach to material testing and structural analysis". PhD thesis. Chalmers University of Technology. ISBN: 9172916966.

Michel, A., Pease, B. J., Geiker, M. R., Stang, H., and Olesen, J. F. (2011). "Monitoring reinforcement corrosion and corrosion-induced cracking using non-destructive x-ray attenuation measurements". In: *Cement and Concrete Research* 41.11, pp. 1085–1094. ISSN: 00088846. DOI: 10.1016/j.cemconres.2011.06.006.

Mihashi, H., Faiz, S., Ahmed, U., and Kobayakawa, A. (2011). "Corrosion of Reinforcing Steel in Fiber Reinforced Cementitious Composites". In: *Journal of Advanced Concrete Technology* 9.2, pp. 159–167.

Naaman, A. E. and Reinhardt, H. W. (2006). "Proposed classification of HPFRC composites based on their tensile response". In: *Materials and Structures* 39.5, pp. 547–555. ISSN: 1359-5997. DOI: 10.1617/s11527-006-9103-2.

Naaman, A. E. (2003). "Engineered Steel Fibers with Optimal Properties for Reinforcement of Cement Composites". In: *Journal of Advanced Concrete Technology* 1.3, pp. 241–252. ISSN: 1346-8014. DOI: 10.3151/jact.1.241.

Nilsson, L.-O. (2001). *Prediction models for chloride ingress and corrosion initiation in concrete structures*. Tech. rep. Nordic Mini Seminar & fib TG 5.5 meeting, Göteborg, May 22-23: Chalmers University of Technology.

Nilsson, L.-O., Poulsen, E., Sandberg, P., Sorensen, H., and Klinghoffer, O. (1996). *HETEK, Chloride penetration into concrete, State of the Art. Report No.53*. Tech. rep. Road Directorate. Denmark Ministry of Transport.

Nilsson, L.-O., Sandberg, P., Poulsen, E., Tang, L., Andersen, A., and Frederiksen, J. (1997). *HETEK, A system for estimation of chloride ingress into concrete, Theoretical background. Report No.83*. Tech. rep. Road Directorate. Denmark Ministry of Transport.

Nordström, E. (2005). "Durability of Sprayed Concrete Steel fibre corrosion in cracks". PhD thesis. LuleåUniversity of Technology.

NT Build 443 (1995). *North Test BUILD 443 - Accelerated chloride Penetration*. Tech. rep., pp. 1–5.

NT Build 492 (1999). *North Test BUILD 492 - Chloride Migration Coefficient from Non-Steady-State Migration Experiments*. Tech. rep., pp. 1–8.

Page, C. L. and Treadaway, K. W. J. (1982). "Aspects of the electrochemistry of steel in concrete". In: *Nature* 297.13 May, pp. 109–115.

Pawlick, L., Stoner, G., and Clemeña, G. (1998). *Development of an embeddable reference electrode for reinforced concrete structures*. Tech. rep. Virginia Transportation Research Council, p. 93.

Pease, B. (2010). "Influence of concrete cracking on ingress and reinforcement corrosion". PhD thesis. Technical University of Denmark. ISBN: 9788778773128.

Pourbaix, M. (1973). *Lectures on Electrochemical Corrosion*. Boston, MA: Springer US, p. 352. ISBN: 978-1-4684-1808-8. DOI: 10.1007/978-1-4684-1806-4.

Poursaee, A. and Hansson, C. M. (2008). "The influence of longitudinal cracks on the corrosion protection afforded reinforcing steel in high performance concrete". In: *Cement and Concrete Research* 38.8-9, pp. 1098–1105. ISSN: 00088846. DOI: 10.1016/j.cemconres.2008.03.018.

Sadeghi-pouya, H., Ganjian, E., Claisse, P., and Muthuramalingam, K. (2013). "Corrosion durability of high performance steel fibre reinforced concrete". In: *Third International Conference on Sustainable Construction Materials and Technologies*. Kyoto, Japan - August 18-21.

Sandberg, P. (1998). "Chloride initiated reinforcement corrosion in marine concrete". PhD thesis. Lund University, p. 86.

Schiessl, P. and Raupach, M. (1997). "Laboratory Studies and Calculations on the Influence of Crack Width on Chloride-Induced Corrosion of Steel in Concrete". In: *ACI Materials Journal* 94.1, pp. 56–61.

Serna, P. and Arango, S. E. (2008). "Evolution of the Flexural Behaviour of Precracked SFRC in Marine Environment". In: *7th RILEM International Symposium on Fibre Reinforced Concrete: Design and Applications - BEFIB 2008*. Chennai, India - September 17-19, pp. 595–605.

Silva, N. (2013). "Chloride Induced Corrosion of Reinforcement Steel in Concrete. Threshold Values and Ion Distributions at the Concrete-Steel Interface". PhD thesis. Chalmers University of Technology, Gothenburg, Sweden. ISBN: 9789173858083.

Solgaard, A. O. S., Geiker, M., Edvardsen, C., and Küter, A. (2013). "Observations on the electrical resistivity of steel fibre reinforced concrete". In: *Materials and Structures* 47.1-2, pp. 335–350. ISSN: 1359-5997. DOI: 10.1617/s11527-013-0064-y.

Someh, A. K. and Saeki, N. (1997). "The Role of Galvanized Steel Fibers in Corrosion-Protection of Reinforced Concrete". In: *Proceedings of Japan Concrete Institute* 19.1, pp. 889–894.

Song, H. and Saraswathy, V. (2007). "Corrosion Monitoring of Reinforced Concrete Structures-A". In: *Int. J. Electrochem. Sci* 2, pp. 1–28.

Švec, O., Žirgulis, G., Bolander, J. E., and Stang, H. (2014). "Influence of formwork surface on the orientation of steel fibres within self-compacting concrete and on the mechanical properties of cast structural elements". In: *Cement and Concrete Composites* 50, pp. 60–72. ISSN: 09589465. DOI: 10.1016/j.cemconcomp.2013.12.002.

Tammo, K. (2009). "A new approach to crack control for reinforced concrete. An investigation of crack widths close to the reinforcement and the correlation to service life". PhD thesis. Lund University, Sweden, p. 81.

Tang, L. (2008). "Engineering expression of the ClinConc model for prediction of free and total chloride ingress in submerged marine concrete". In: *Cement and Concrete Research* 38.8-9, pp. 1092–1097. ISSN: 00088846. DOI: 10.1016/j.cemconres.2008.03.008.

Tang, L., Fu, Y., and León, A. (2010). *Rapid Assessment of Reinforcement Corrosion in Concrete Bridges*. Tech. rep. CBI Betonginstitutet, p. 88.

Tang, L., Nilsson, L.-O., and Basheer, P. A. M. (2012). *Resistance of Concrete to Chloride Ingress Testing and modelling*. Spon Press, p. 259.

Tuutti, K. (1982). "Corrosion of steel in concrete". In: *CBI Report 4:82, The Swedish Cement and Cocnrete Institute*. P. 468.

Uji, K., Matsuoka, Y., and Maruya, T. (1990). "Formulation of an equation for surface chloride content of concrete due to permeation of chloride". In: *Proceedings of the Third International Symposium on "Corrosion of Reinforcement in Concrete Construction"*. Wishaw, Warwickshire, pp. 258–267.

Vidal, T., Castel, A., and François, R. (2004). "Analyzing crack width to predict corrosion in reinforced concrete". In: *Cement and Concrete Research* 34.1, pp. 165–174. ISSN: 00088846. DOI: 10.1016/S0008-8846(03)00246-1.

Vidal, T., Castel, A., and François, R. (2007). "Corrosion process and structural performance of a 17 year old reinforced concrete beam stored in chloride environment". In: *Cement and Concrete Research* 37.11, pp. 1551–1561. ISSN: 00088846. DOI: 10.1016/j.cemconres.2007.08.004.

Vitt, G. (2008). "Combined reinforcement - practical experiences". In: *7th RILEM International Symposium on Fibre Reinforced Concrete: Design and Applications - BEFIB 2008*, pp. 1021–1028.

Yoon, S., Wang, K., Weiss, W., and Shah, S. (2000). "Interaction between loading, corrosion, and serviceability of reinforced concrete". In: *ACI materials journal* 97.6, pp. 637–644.

Appendices

Appendix A:
Half-cell potential measurements

In this appendix the complete set of half-cell potential measurements during a period of one year is included for all the monitored reinforcing bars in the different series and for all the loading conditions.

To ease the reference to the different specimens and facilitate the interpretation of results to the reader, the following nomenclature is introduced:

XX00Y99Z

where:

- XX: Refers to the different series: plain (PL), steel (ST), hybrid (HY) and synthetic (SY).
- 00: Represents an identification number for each beam within the series.
- XY: Indicates the loading conditions: non-cracked (N), unloaded (U), cyclically loaded (C) and loaded (L).
- 99: Specifies the target crack width during the pre-loading procedure in millimetres: 01, 02, 03 or 04.
- Z: Refers to the position of a specific reinforcement bar in the corresponding specimen, being either central (C) or external (E).

Half-cell potential for *Uncracked* beams in the *plain* series

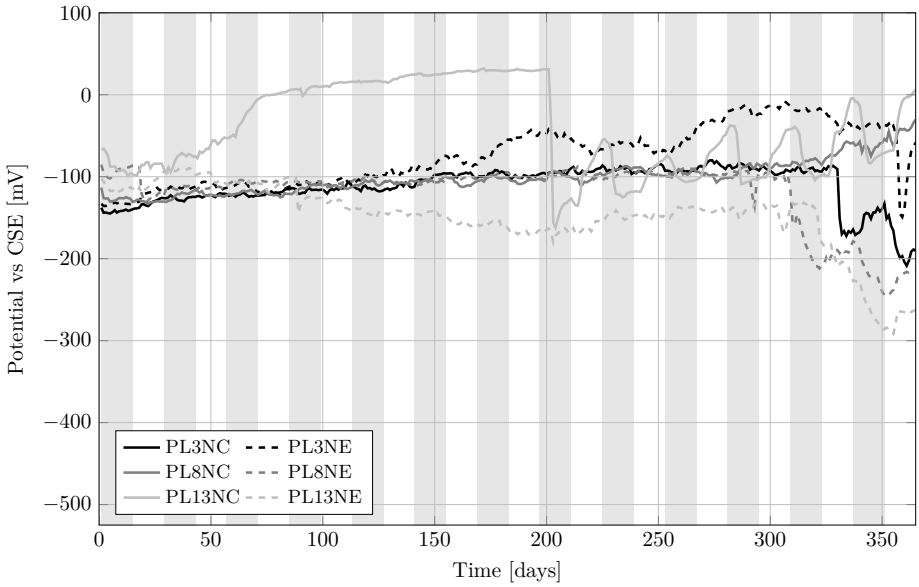

Half-cell potential for *Uncracked* beams in the *steel* series

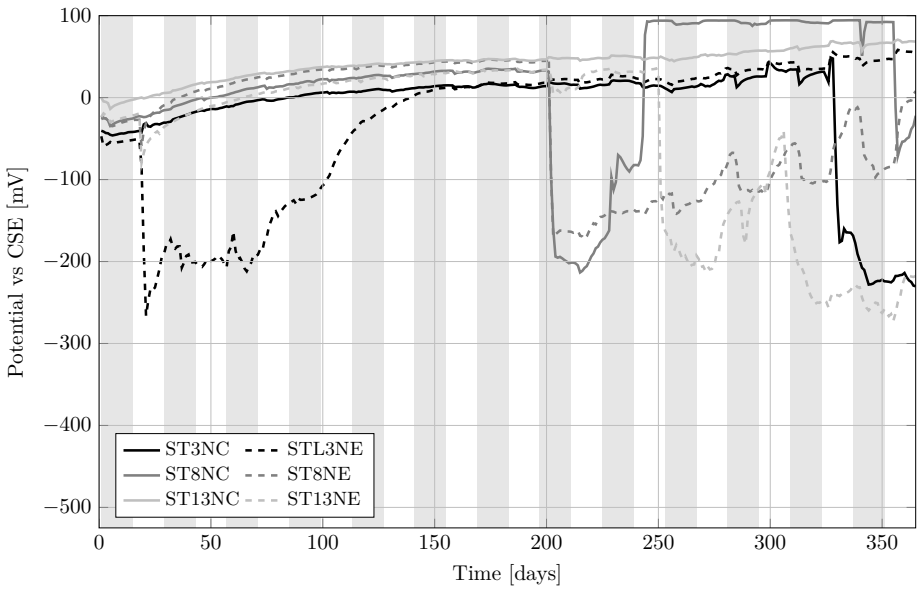

Half-cell potential for *Uncracked* beams in the *hybrid* series

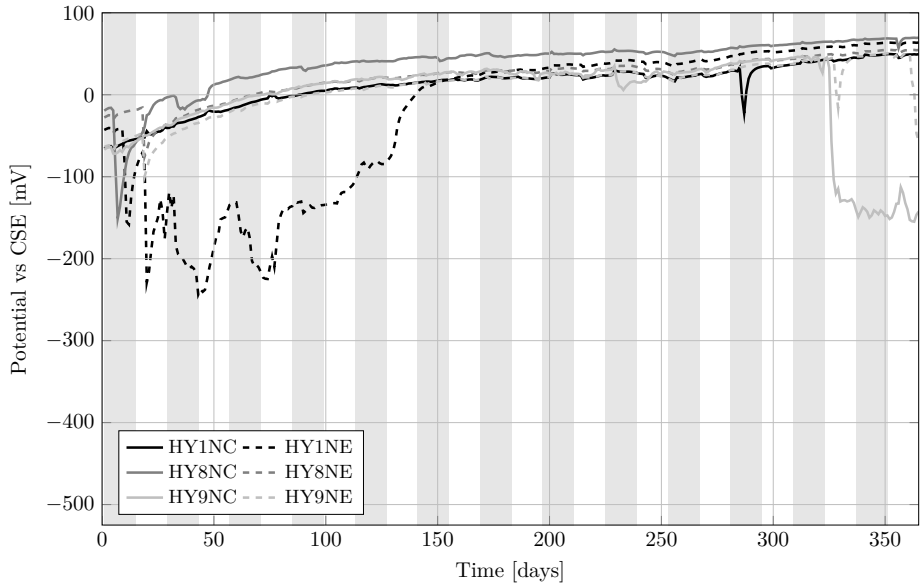

Half-cell potential for *Uncracked* beams in the *synthetic* series

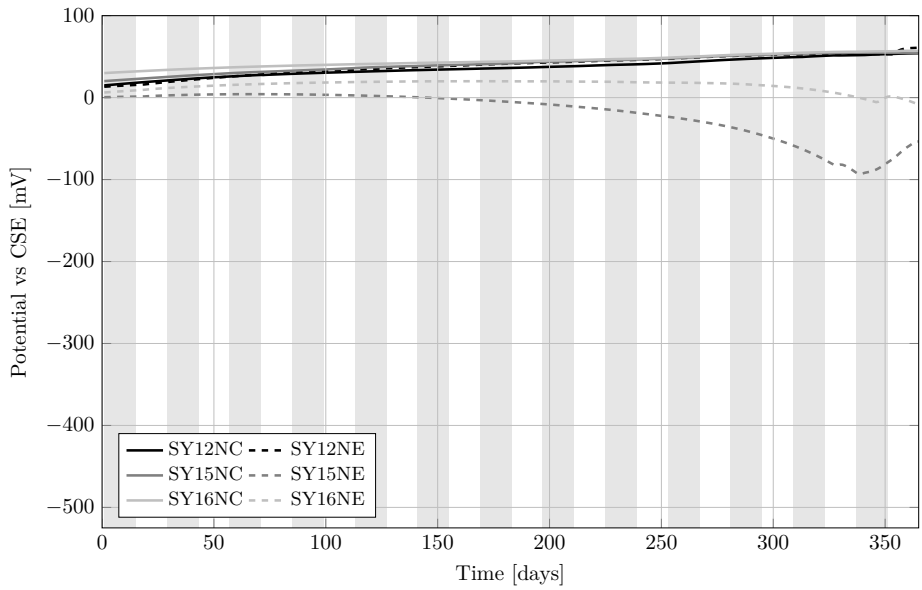

Half-cell potential for *Unloaded* beams in the *plain* series

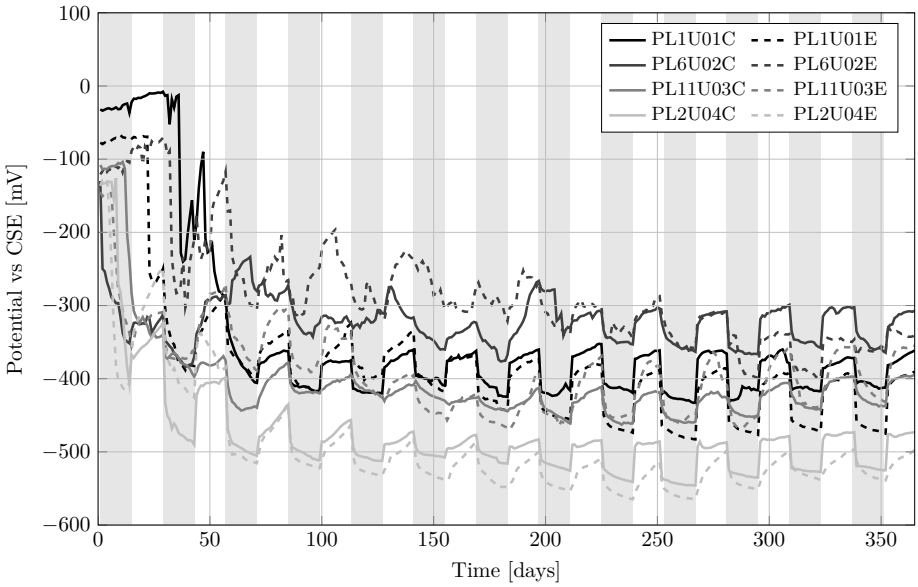

Half-cell potential for *Unloaded* beams in the *steel* series

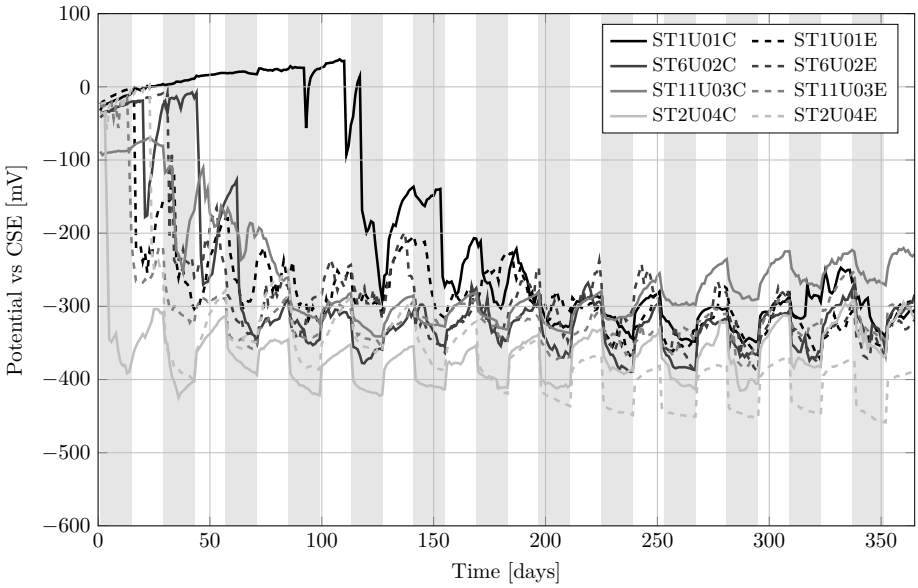

Half-cell potential for *Unloaded* beams in the *hybrid* series

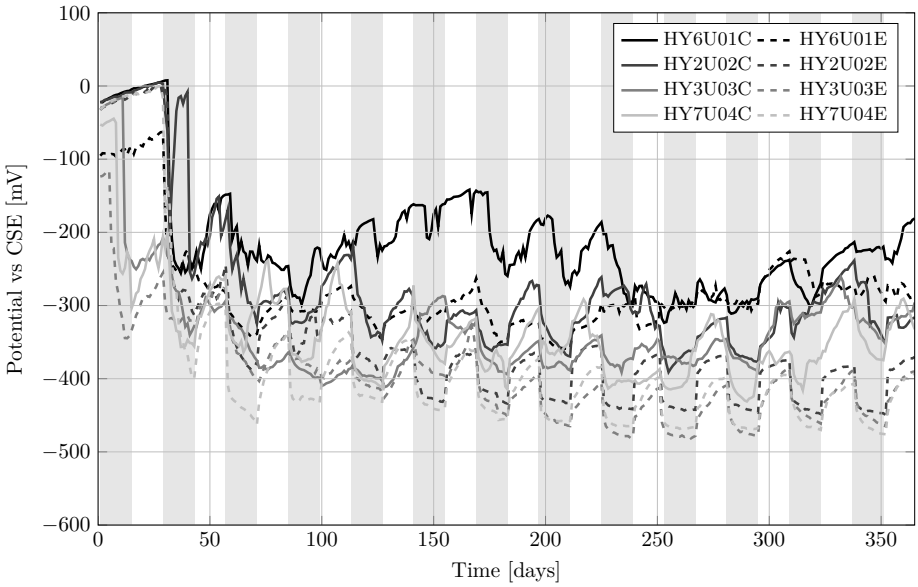

Half-cell potential for *Unloaded* beams in the *synthetic* series

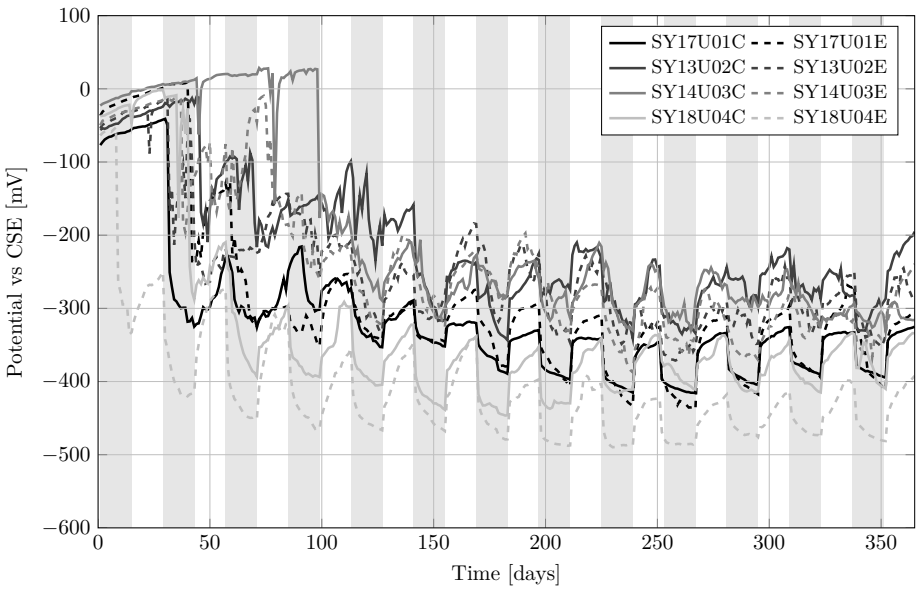

Half-cell potential for *Cyclically loaded* beams in the *plain* series

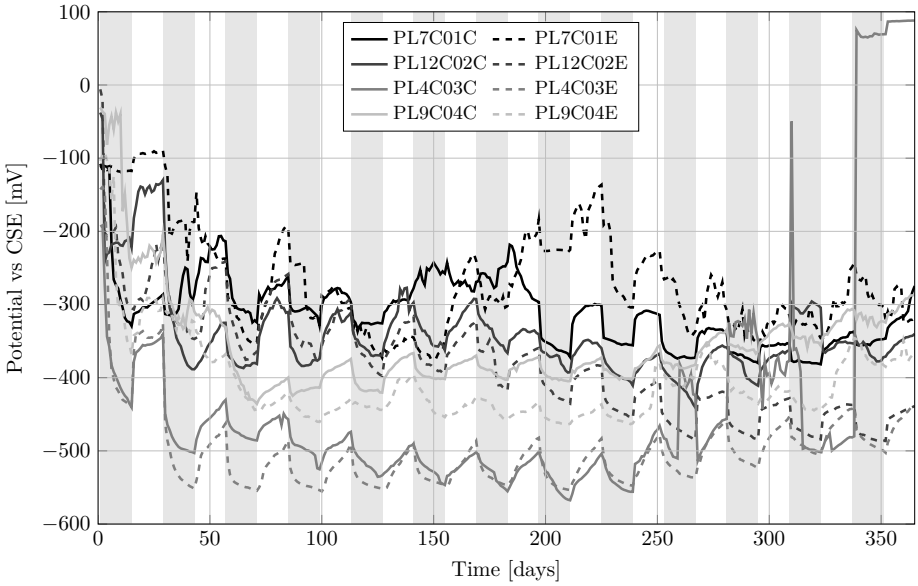

Half-cell potential for *Cyclically loaded* beams in the *steel* series

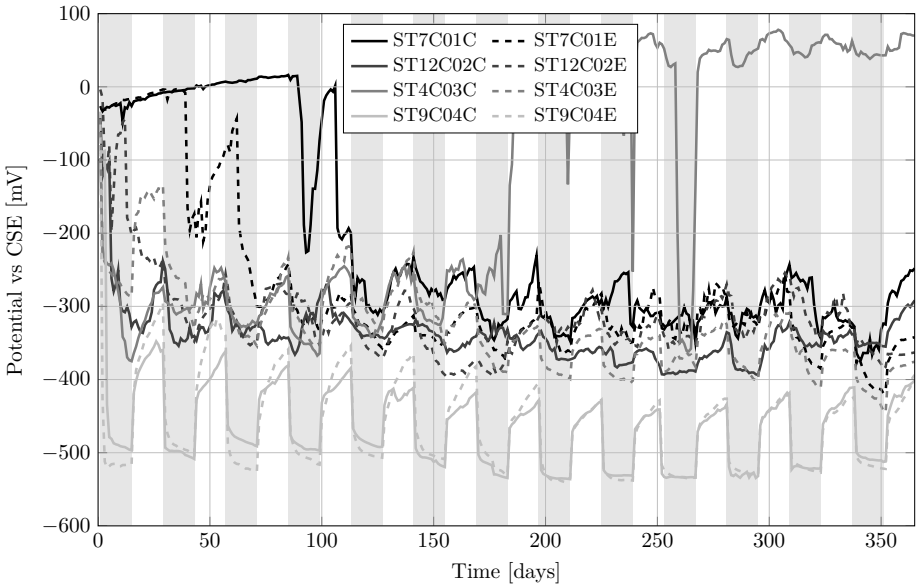

Half-cell potential for *Cyclically loaded* beams in the *hybrid* series

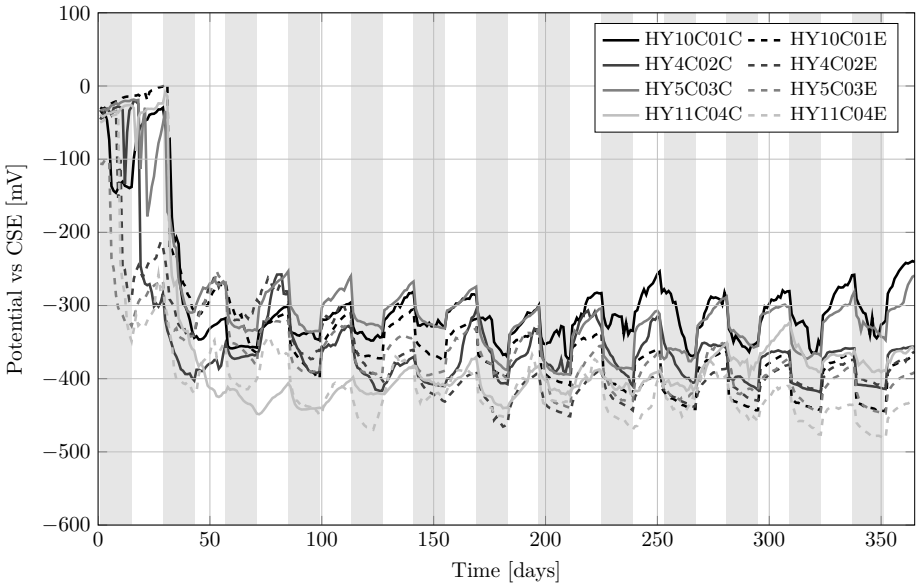

Half-cell potential for *Loaded* beams in the *plain* series

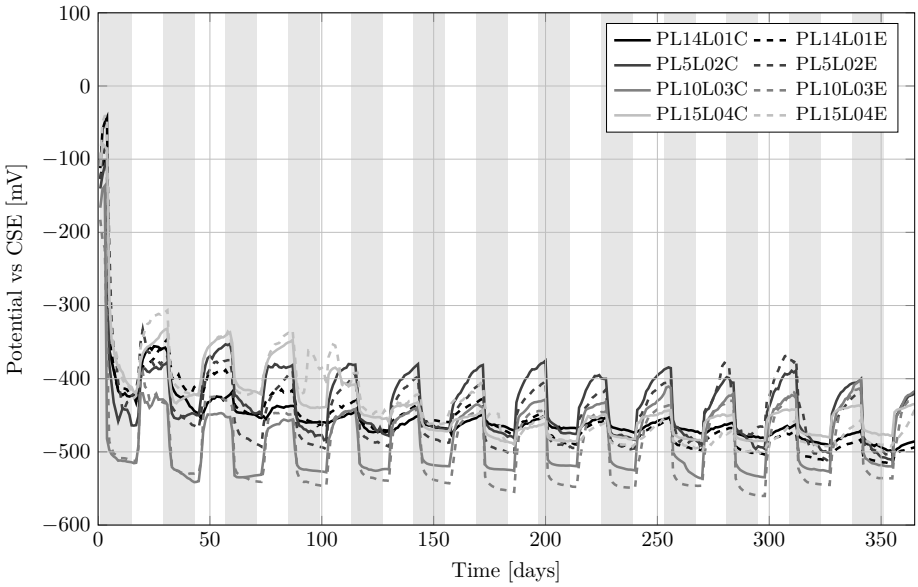

Half-cell potential for *Loaded* beams in the *steel* series